Accurate and Complete Genomes from Metagenomes

Lin-Xing Chen[1], Karthik Anantharaman[1,7], Alon Shaiber[2,3], A. Murat Eren[3,4,*], and Jillian F. Banfield[1,5,6*]

[1] Department of Earth and Planetary Sciences, Berkeley, CA, USA.
[2] Graduate Program in Biophysical Sciences, University of Chicago, Chicago, IL 60637, USA.
[3] Department of Medicine, University of Chicago, Chicago 60637 IL, USA.
[4] Bay Paul Center, Marine Biological Laboratory, Woods Hole 02543 MA, USA.
[5] Department of Environmental Science, Policy, and Management, Berkeley, CA, USA.
[6] Earth and Environmental Sciences, Lawrence Berkeley National Laboratory, Berkeley, CA, USA.
[7] Present address: Department of Bacteriology, University of Wisconsin, Madison, WI, USA.

*Corresponding authors:
Email: jbanfield@berkeley.edu
Telephone: 510-316-4334
Address: McCone Hall, Berkeley, CA 94720

Email: a.murat.eren@gmail.com
Telephone: 773-702-5935
Address: 900 E. 57th St., Chicago, IL 60637 USA

Running title: Curated and complete metagenome-assembled genomes

Abstract

Genomes are an integral component of the biological information about an organism and, logically, the more complete the genome, the more informative it is. Historically, bacterial and archaeal genomes were reconstructed from pure (monoclonal) cultures and the first reported sequences were manually curated to completion. However, the bottleneck imposed by the requirement for isolates precluded genomic insights for the vast majority of microbial life. Shotgun sequencing of microbial communities, referred to initially as community genomics and subsequently as genome-resolved metagenomics, can circumvent this limitation by obtaining metagenome-assembled genomes (MAGs), but gaps, local assembly errors, chimeras and contamination by fragments from other genomes limit the value of these genomes. Here, we discuss genome curation to improve and in some cases achieve complete (circularized, no gaps) MAGs (CMAGs). To date, few CMAGs have been generated, although notably some are from very complex systems such as soil and sediment. Through analysis of ~7000 published complete bacterial isolate genomes, we verify the value of cumulative GC skew in combination with other metrics to establish bacterial genome sequence accuracy. Interestingly, analysis of cumulative GC skew identified potential mis-assemblies in some reference genomes of isolated bacteria and the repeat sequences that likely gave rise to them. We discuss methods that could be implemented in bioinformatic approaches for curation to ensure that metabolic and evolutionary analyses can be based on very high-quality genomes.

Keywords: Metagenomics; complete genomes; genome curation; GC skew

Introduction

In an opinion paper published relatively early in the microbial genomics era, Fraser et al. stated "you get what you pay for" (Fraser et al. 2002). The authors argued the lower scientific value of draft (partial) vs. complete genomes, noting for example higher error rates, potential contaminant sequences, loss of information about gene order, lower ability to distinguish additional chromosomes and plasmids, and most importantly, missing genes. Despite the clarity of this view, the field moved toward the generation of draft isolate genomes to optimize the rate of supply of new sequence information and to lower the cost. Genome-resolved metagenomics has almost exclusively settled for uncurated draft genomes, now often referred to as metagenome-assembled genomes (MAGs). A summary of the basic methods for generating MAGs was provided by (Sangwan et al. 2016). A more recent review provides an overview of assembly methods and offers some insights into the complexity of genome recovery from metagenomes and a valuable overview of certain types of assembly errors that can occur (Olson et al. 2017).

The first MAGs were published in 2004 (Tyson et al. 2004) and there are now hundreds of thousands of them in public databases. The ever increasing depth of high-throughput sequencing now make even the most challenging environments with low archaeal, bacterial, and viral biomass, such as insect ovaries (Reveillaud et al. 2019), human gut tissue biopsies (Vineis et al. 2016), hospital room surfaces (Brooks et al. 2017), and even human blood (Moustafa et al. 2017) amenable to shotgun metagenomic surveys and recovery of MAGs. Although incomplete, draft MAGs represent a major advance over knowing nothing about the genes and pathways present in an organism, and led to the discovery of new metabolisms. For example, the complete oxidation of ammonia to nitrate via nitrite (i.e., comammox) was determined by the detection of necessary genes in a single MAG (Daims et al. 2015; van Kessel et al. 2015). MAGs are often derived from uncultivated organisms that can be quite distantly related to any isolated species, which is a clear advantage of MAGs (Becraft et al. 2017; Garg et al. 2019). For this reason, genome-resolved metagenomics has been critical for more comprehensive descriptions of bacterial and archaeal diversity and the overall topology of the Tree of Life (Hug et al. 2016).

Counter to this view, there is some sentiment that MAGs are not useful because they are composites and thus not representative of their populations (Becraft et al. 2017). However, a genome reconstructed from a clonal microbial culture also does not represent the cloud of biologically important variation that exists in the natural population from where the isolate was derived. Population diversity can be analyzed by comparing all individual sequences (or short reads) to the metagenome-assembled reference

genome (Simmons et al. 2008; Delmont et al. 2019). While some populations are near-clonal, others are very complex strain mixtures and yet others fall on the continuum between these (Lo et al. 2007; Chivian et al. 2008; Simmons et al. 2008). As strain divergence leads to assembly fragmentation (expanded on below), high quality genomes are unlikely to be generated for relatively heterogeneous populations. Assembly of exceptionally long fragments from short read (e.g., Illumina) data is only anticipated when within population diversity is low, as may occur following a recent bloom, selective sweep, or due to recent colonization by a single cell or a small cluster of closely related cells. In such cases, the genomes that assemble well are typically highly representative of the population from which they are derived and the vast majority of reads report the same base at the same position. For example, in one recently published complete 4.55 Mbp genome (Banfield et al. 2017), the frequency of single nucleotide variants (SNVs) is ~ 0.12% (Figure 1), not substantially different from the expected sequencing error rate (0.04-0.12%) (Schirmer et al. 2016).

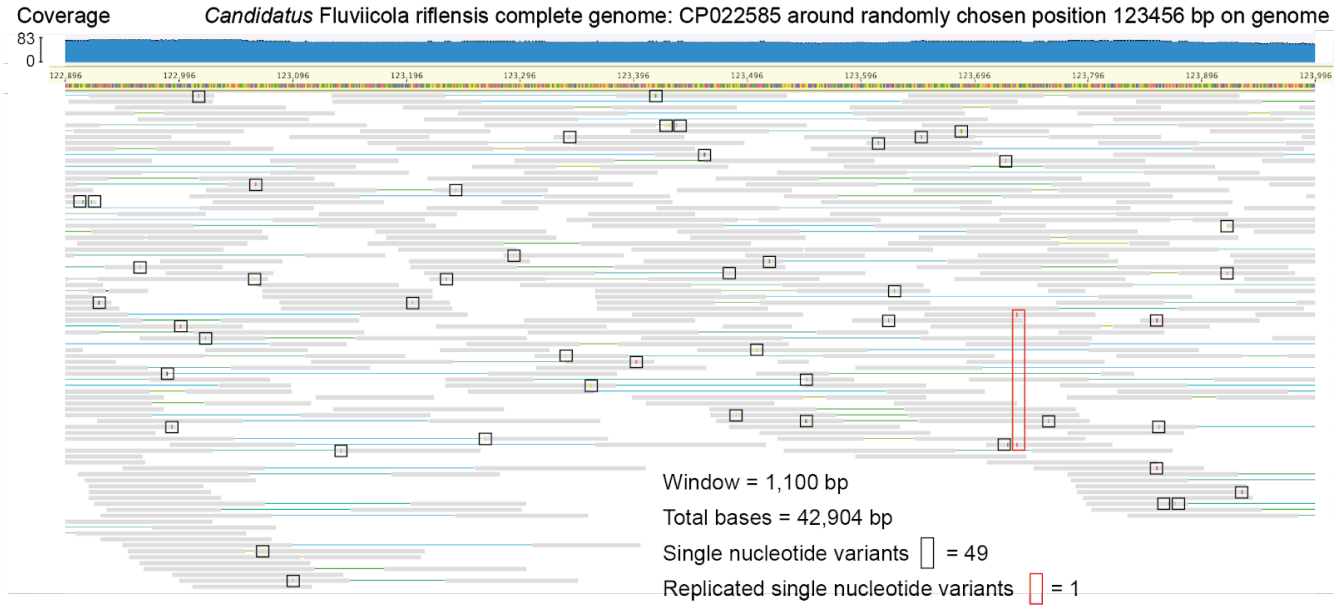

Figure 1. The low frequency of single nucleotide variants (SNVs) of a recently published CMAG. A randomly chosen region, centered on position 123,456 (1100 bp in length) of the CMAG of *Candidatus* Fluviicola riflensis is shown with mapped reads (Banfield et al. 2017). SNVs that only occur once are indicated by black boxes and the one replicated SNV indicated by a red box. Clearly, the consensus sequence is well supported.

Assembly and binning are important steps in metagenomic studies

Assembly of short metagenomic reads into contiguous segments of DNA is a computationally intensive task, and its effectiveness often depends on the complexity of the environment (Sharon and Banfield 2013). However, assembly of contigs/scaffolds offers many advantages over short-read based analyses. First, they enable the identification of complete open reading frames. Second, assemblies provide larger genomic contexts (e.g., operons). In combination, these considerations improve predictions of metabolic capacities. Further, assembled sequences provide information about gene synteny and better resolve taxonomic profiles (e.g., by providing sets of proteins for taxonomy based on concatenated proteins encoded in the same genome (e.g., (Hug et al. 2016; Parks et al. 2018)). These improvements can overcome misleading interpretations of short-read data (Ackelsberg et al. 2015; Afshinnekoo et al. 2015).

The critical step required to establish a genome from a metagenomic assembly is binning. This involves assignment of assembled fragments to a draft genome based on detection on any scaffold of some signal(s) that occur(s) locally within a genome and persists genome-wide. Most commonly used features that can facilitate accurate binning of scaffolds include depth of sequencing measured by read coverage, sequence composition measured for example by tetranucleotide composition, and phylogenetic profile measured by the

135 ‘best taxonomic hits’ for each predicted protein on each scaffold. Sometimes, and mostly in datasets from very
136 simple communities or for highly abundant organisms, the process of binning can be as easy as collecting
137 together all fragments that share a single clearly defined feature (Figure S1), such as a discrete set of scaffolds
138 with similar coverage, or unique and well-defined tetranucleotide patterns or GC content. In other cases, a
139 combination of a few well defined signals, such as GC content, coverage, and phylogenetic profile of scaffolds,
140 are sufficient to clearly define a bin. However, over reliance on phylogenetic profile can be dangerous,
141 especially if the genome is for an organism that is only distantly related to those in the databases used for
142 profiling. Further, some fragments can have an unexpected phylogenetic profile relative to the rest of the
143 genome because the region has not been encountered previously in genomes of related organisms, possibly
144 because it was acquired by lateral gene transfer. Thus, the most robust bins will draw on a combination of
145 multiple clear signals.
146 If a study includes a set of samples with related community membership, an important constraint
147 for bin assignment can be provided by the shared patterns of abundance of a fragment across a sample series.
148 The use of series samples data for binning was first proposed by Sharon et al. (Sharon et al. 2013), and this
149 strategy is now a central feature in most automated binning algorithms, including CONCOCT (Alneberg et al.
150 2013), MaxBin (Wu et al. 2014), ABAWACA (Brown et al. 2015) and MetaBAT (Kang et al. 2015), as well as
151 manual binning and MAG refinement strategies (Wrighton et al. 2012; Shaiber and Eren 2019). Series based
152 binning can exclude contaminant scaffolds from a MAG whose abundance shows a different pattern over
153 time/space/treatment. We have found that no single binning algorithm is the most effective for all
154 sample/environment types or even for all populations within one sample. The recently published method
155 DASTool tests a flexible number of different binning methods, evaluates all outcomes and chooses the best bin
156 for each population (Sieber et al. 2018). A similar strategy has been utilized in a modular pipeline software
157 called MetaWRAP (Uritskiy et al. 2018).
158
159 **A case study: Binning can greatly improve data interpretation**
160 Contigs that do not represent entire chromosomes may not be appropriate proxies for microbial populations
161 without binning, and claims made based on unbinned contigs can lead to erroneous conclusions. For instance,
162 a recent study focusing on human blood used shotgun metagenomic sequencing of circulating cell-free DNA
163 from more than 1,000 samples and recovered a large number of contigs with novel bacterial and viral
164 signatures (Kowarsky et al. 2017), suggesting that "hundreds of new bacteria and viruses" were present in
165 human blood, and that this environment contained more microbial diversity than previously thought. While the
166 authors performed PCR experiments to independently confirm the existence of some of these signatures in
167 blood samples, they did not attempt to assign assembled contigs to genome bins. Here, we studied contigs
168 from these blood metagenomes with a genome-resolved strategy to investigate the presence of previously
169 unknown bacterial populations.
170 To explore the origin of bacterial signatures found in the novel set of contigs recovered from cell-
171 free DNA blood metagenomes (Figure 2a), we first searched for the 139 bacterial single-copy core genes (SCGs)
172 described by Campbell et al. (Campbell et al. 2013). This analysis identified 76 bacterial SCGs among all contigs,
173 and of these, 56 occurred only once, suggesting that a single microbial population may explain a large fraction
174 of the bacterial signal found among novel contigs (Figure 2b). Of the 56 genes that occurred only once, 18 were
175 ribosomal proteins. Comparison of the amino acid sequences of these ribosomal proteins to those in the NCBI’s
176 non-redundant protein sequence database revealed that the vast majority of them best matched to proteins
177 from genomes that fall within the recently described 'Candidate Phyla Radiation' (CPR) (Brown et al. 2015), a
178 group of microbes with rather small genomes, reduced metabolic capacities (Rinke et al. 2013; Brown et al.
179 2015), and at least in some cases very small cell sizes (Luef et al. 2015), which suggest largely symbiotic
180 lifestyles (He et al. 2015; Nelson and Stegen 2015). Even though ribosomal proteins found in blood
181 metagenomes best matched to CPR genomes, the levels of sequence identity of these matches were very low,
182 and taxonomic affiliations of best hits were divergent within the CPR (Table S1), which could simply reflect the
183 novelty of a single population rather than the presence of multiple populations. To investigate the distribution
184 of these proteins we clustered novel contigs based on their tetranucleotide frequencies (Figure 2a). We found

185 that most bacterial SCGs occurred in a relatively small group of contigs with similar tetranucleotide
186 composition. Manual selection of these contigs, and their further refinement using additional 'non-novel'
187 contigs that were not included in the original study by Kowarsky et al. (2017) resulted in a single CPR MAG that
188 is 613.5 kbp in size with a completion estimate of 52.5%. Our phylogenomic analysis affiliated this MAG with
189 the superphylum Parcubacteria (previously OD1) of the CPR (Figure 2c). Regardless of the origins of this
190 population in these metagenomes, our genome-resolved analysis contrasts with the prior interpretation of
191 these data and suggests that Parcubacteria appears to be the only major novel bacterial group whose DNA is
192 present in human blood metagenomes. This finding demonstrates the critical importance of binning-based
193 strategies to justify claims of microbial diversity in metagenomic analyses.
194

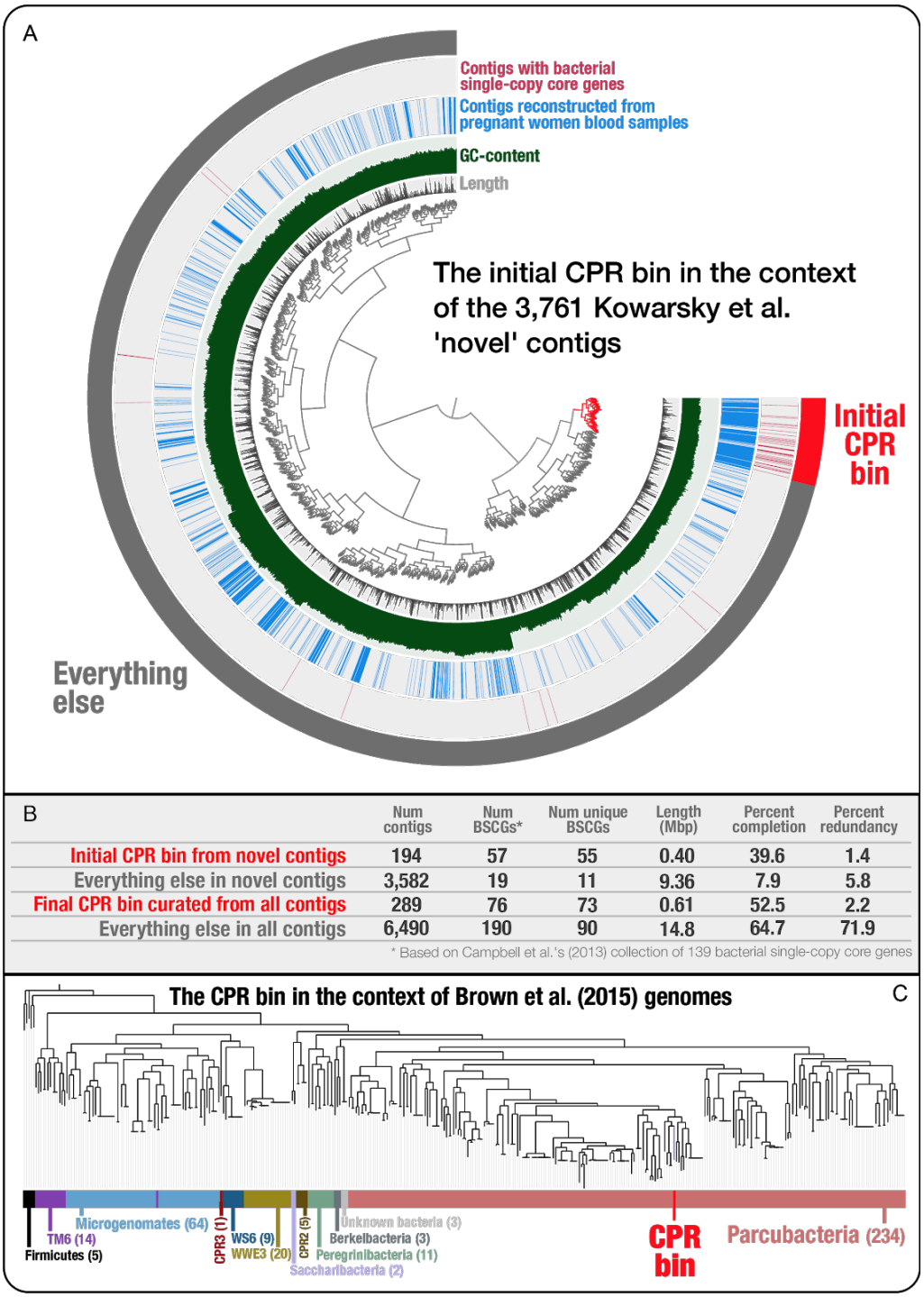

	Num contigs	Num BSCGs*	Num unique BSCGs	Length (Mbp)	Percent completion	Percent redundancy
Initial CPR bin from novel contigs	194	57	55	0.40	39.6	1.4
Everything else in novel contigs	3,582	19	11	9.36	7.9	5.8
Final CPR bin curated from all contigs	289	76	73	0.61	52.5	2.2
Everything else in all contigs	6,490	190	90	14.8	64.7	71.9

* Based on Campbell et al.'s (2013) collection of 139 bacterial single-copy core genes

195

196 **Figure 2**. **Genome-resolved metagenomics is essential to better predict microbial diversity.** (A) The inner
197 dendrogram in Panel A displays the hierarchical clustering of 3,761 'novel' Kowarsky et al. contigs based on
198 their tetranucleotide frequency (using Euclidean distance and Ward clustering). While the two inner layers
199 display the length and GC-content of each contig, the outer two layers mark each contig that originates from
200 the assemblies of pregnant women blood samples, and the ones that contain one or more bacterial single-copy
201 core genes. Panel B compares the initial CPR bin and the remaining contigs in the 'novel' set, as well as the final
202 CPR bin and the remaining contigs in the entire assembly (which contains both novel and non-novel contigs).
203 Panel C shows the placement of the CPR bin in the context of CPR genomes released by Brown et al. (2015).
204 See http://merenlab.org/data/parcubacterium-in-hbcfdna/ for more details on this case study.
205
206 **Yet, binning can be an important source of error**
207 A real danger is that conclusions from draft MAGs may be incorrect due to misbinning (the wrong assignment
208 of a genome fragment from one organism to another). It is critical to not rely on MAGs with high levels of
209 contamination as these will likely yield misleading evolutionary and ecological insights (Bowers et al. 2017;
210 Shaiber and Eren 2019). Misbinning is especially likely if scaffolds are short (e.g., < 5 kbp), where binning signals
211 can be noisy or unreliable. Thus, for better binning performance, it is helpful to use an assembler that includes
212 a scaffolding step (insertion of Ns in gaps between contigs spanned by paired-end reads), such as IDBA_UD
213 (Peng et al. 2012), or metaSPAdes (Nurk et al. 2017). MAGs can also be screened for short scaffolds with, for
214 example, erroneous rRNA genes, which are often misbinned due to their anomalous coverage (especially if the
215 scaffolds are short and the genes are present in multicopy). Bins may also be contaminated by phage and
216 plasmid genome fragments with coincidentally similar coverage or GC content etc.
217 Completeness and contamination are often estimated using the inventory of expected SCGs in a
218 MAG. A set of SCGs is selected based on their presence in all bacterial genomes, or at least all genomes within
219 a taxonomic group (identified based on the phylogeny). In a genome without contamination they should be
220 present without redundancy. A widely used tool to assay both completeness and contamination is CheckM
221 (Parks et al. 2015), although other methods are in use (Eren et al. 2015; Anantharaman et al. 2016). It has been
222 noted both in the original study and in subsequent studies that CheckM can generate a false sense of bin
223 accuracy, as demonstrated by combining two partial single-cell genome bins (Parks et al. 2015; Becraft et al.
224 2017). The absence of multiple copies of SCGs does not preclude the presence of fragments from unrelated
225 organisms that will compromise the biological value of the MAGs. While there are tools for interactive
226 visualization of genome bins in a single sample (Laczny et al. 2015; Raveh-Sadka et al. 2015) or across multiple
227 samples (Eren et al. 2015) that enable manual curation opportunities to identify contamination beyond SCG-
228 based estimates, the scalability of this strategy is limited. For example, recently there have been reports of
229 many thousands, even hundreds of thousands, of draft MAGs from public metagenomic datasets (Parks et al.
230 2017; Almeida et al. 2019; Nayfach et al. 2019; Pasolli et al. 2019). Such large-scale analyses often rely on
231 simplified procedures, e.g., coverage profile of a single sample for binning, use of a single binning algorithm,
232 completeness/contamination estimates based on SCG inventories. As these genomes are readily adopted by
233 the scientific community for a wide variety of investigations, errors due to misbinning will propagate.
234
235 **A case study: SCGs can fail to predict the quality of MAGs**
236 In a recent publication, Pasolli et al. used a single-sample assembly approach combined with automatic binning
237 to generate 345,654 MAGs from the human microbiome, of which 154,723 pass a completion and quality
238 threshold based on SCGs (Pasolli et al. 2019). The authors suggest that the quality of the MAGs they have
239 reconstructed through this pipeline was comparable to the quality of genomes from bacterial isolates or MAGs
240 that were manually curated (Pasolli et al. 2019). However, reconstructing MAGs from single metagenomes and
241 the heavy reliance on SCGs to estimate their quality can yield misleading results.
242 We examined one of the Pasolli et al. MAGs, 'HMP_2012__SRS023938__bin.39' (Pasolli et al. 2019)
243 (hereafter referred to as Pasolli MAG), which resolves to the candidate phylum Saccharibacteria (formerly
244 known as TM7), a poorly understood branch of the Tree of Life that contains members that are common in the
245 human oral cavity (Bor et al. 2019). This MAG, 897,719 bp in length with 57 contigs (N50: 34,012 bp) (Table S2),

246 was recovered by Pasolli et al. from a supragingival plaque sample (experiment accession: SRR060355; sample
247 accession: SRS023938) collected and sequenced by the Human Microbiome Project (HMP) (Turnbaugh et al.
248 2007). Anvi'o estimated the Pasolli MAG to include 84% of bacterial SCGs with very low redundancy (2.8%), in
249 comparison, CheckM reported 63.39% completeness and 0.85% contamination (Table S2).
250 The HMP dataset included two additional plaque metagenomes from the same individual, providing
251 an opportunity to investigate the distribution patterns of contigs binned together in this MAG across multiple
252 samples from the same person through metagenomic read recruitment. Organizing contigs based on their
253 sequence composition and differential coverage patterns across three samples revealed two distinct clusters
254 (Figure 3), the smaller one of which contained 11 contigs that added up to a total length of 53.5 kbp (Figure 3,
255 outer circle: orange). While the average mean coverage of contigs in these clusters were relatively comparable
256 in the metagenome from which the MAG was reconstructed (24.6X vs 31.1X), the average coverages differed
257 more dramatically in the other two plaque metagenomes (99.4X vs 20.7X in SRS013723 and 9.7X vs 33.56X in
258 SRS078738), which suggest that the emergence of these two clusters was due to the improved signal for
259 differential coverage with the inclusion of additional samples (Figure 3). A BLAST search on the NCBI's non-
260 redundant database matched genes found in 10 of 11 contigs in the smaller cluster to genomes of *Veillonella*
261 (belonging to Firmicutes; Table S3), a genus that is common to the human oral cavity (Mark Welch et al. 2014)
262 and includes members that are present in multiple oral sites (Eren et al. 2014). Genes in the remaining contig in
263 the smaller cluster lacked a strong match (contig 000000000028, Table S3), yet best matched to genes in
264 *Selenomonas* genomes instead of Saccharibacteria, suggesting that the smaller cluster represented
265 contamination. As these contaminating contigs did not include any SCGs, their inclusion did not influence SCG-
266 based completeness and contamination estimates. Thus, they remained invisible to the quality assessment.
267 While the contamination in this case will unlikely influence the placement of this particular MAG in the Tree of
268 Life due to the lack of SCGs in it, the contamination does change the functional makeup of the MAG: our
269 annotation of 54 genes in the 11 contaminating contigs using the NCBI's Clusters of Orthologous Groups (COGs)
270 revealed 30 functions that were absent in the MAG after the removal of the contamination (Table S4). In
271 addition to misleading functional profiles, contamination issues often influence ecological insights. Our read
272 recruitment analysis to characterize the distribution of the Pasolli MAG contigs across all 196 plaque and 217
273 tongue metagenomes from 131 HMP individuals showed that while this Saccharibacteria population appears to
274 be restricted to plaque samples, contigs that contaminated this MAG recruited reads also from the tongue
275 samples (Figure 3, Table S5).
276 We did not investigate the quality of the full set of 154,723 MAGs described by Pasolli et al. (Pasolli
277 et al. 2019) or the genomes reported in other studies that relied on similar automated strategies (Almeida et al.
278 2019; Nayfach et al. 2019). Nevertheless, this example demonstrates that SCGs alone cannot predict the lack of
279 contamination in a given MAG or characterize the extent of contamination in genomic collections (see another
280 example in Figure S2). Overall, it is essential for our community to note that computational analyses that rely
281 heavily on SCGs to assess the quality of MAGs can promote erroneous insights.
282

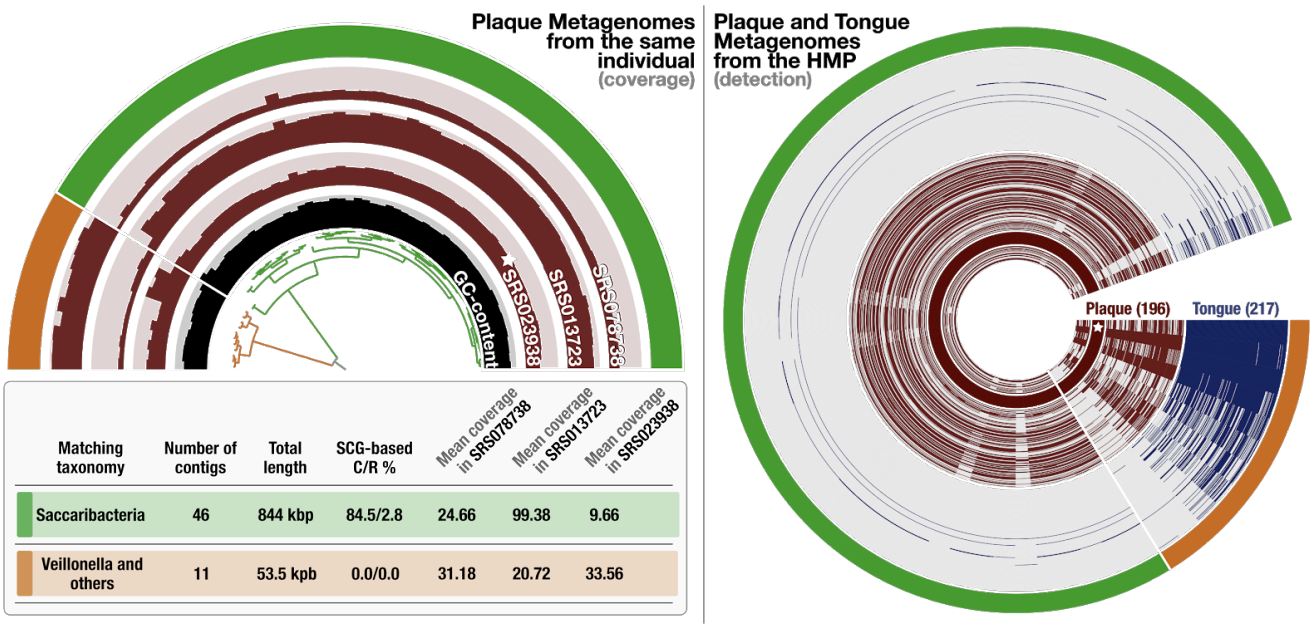

Matching taxonomy	Number of contigs	Total length	SCG-based C/R %	Mean coverage in SRS078738	Mean coverage in SRS013723	Mean coverage in SRS023938
Saccaribacteria	46	844 kbp	84.5/2.8	24.66	99.38	9.66
Veillonella and others	11	53.5 kpb	0.0/0.0	31.18	20.72	33.56

Figure 3. Contamination in MAG without extra copies of SCGs. In the left panel, the half-circle displays the mean coverage of each contig in Pasolli MAG across three plaque metagenomes that belong to the same individual, where the 'star' symbol denotes the sample from which the original MAG was reconstructed. The dendrogram in the center represents the hierarchical clustering of the 57 contigs based on their sequence composition and differential mean coverage across the three metagenomes, while the innermost circle displays the GC-content for each contig. The outermost circle marks two clusters: one with 46 contigs (green) and another one with 11 contigs (orange). The table underneath this display summarizes various statistics about these two clusters, including the best matching taxonomy, total length, completion and redundancy (C/R) estimations based on SCGs, and the average mean coverage of each cluster across metagenomes. In the right panel, the distribution of the same contigs and clusters are shown across 196 plaque (brown) and 217 tongue (blue) metagenomes generated by the Human Microbiome Project (HMP). Each concentric circle in this display represents a single metagenome, and data points display the detection of the contigs in Pasolli MAG.

Genome curation - moving towards complete genomes

The opportunity to recover huge numbers of new genomes from metagenomic datasets motivates the development of new tools to more comprehensively curate draft MAGs, ideally to completion. Although the term 'complete' should be reserved for genome sequences with (usually) circular chromosomes reported in single scaffolds, in contemporary genome-resolved metagenomics studies the term is commonly used to describe bacterial and archaeal genomes that have all the expected SCG markers used to evaluate completeness. This use of the term 'complete' does not exclude genomes that are extremely fragmented, which can suffer from contamination issues, as we demonstrate above. Here we use the term 'complete' explicitly to describe multiple properties of a genome: (1) circular (assuming the chromosome is circular) and single chromosomal sequences, with (2) perfect read coverage support throughout (i.e., the vast majority of bases in mapped reads at any position matches to the consensus base), and (3) no gaps. To avoid any confusion, we will use the term 'CMAGs' to describe complete MAGs that meet the three criteria.

One of the first CMAG appeared in 2008, but this was for a bacterium that comprised > 99.9% of the sample (Chivian et al. 2008). A second genome published in the same year was for a candidate phylum bacterium in a bioreactor and was reconstructed by sequencing of a fosmid library (Pelletier et al. 2008). And the third one was a Elusimicrobia genome reconstructed from Termites gut (Hongoh et al. 2008). It was not until 2012 and 2013 that a series of CMAGs from multi-species natural communities began to appear (Iverson et al. 2012; Castelle et al. 2013; Di Rienzi et al. 2013; Kantor et al. 2013). In most cases, these genomes were

very close to complete upon *de novo* assembly, although some effort was required to finish them. Near complete *de novo* assembly is a very rare outcome, given that most genomes are assembled using short paired-end reads (e.g., 150 bp with a few hundred base pair insert size). However, given that many samples generate hundreds of draft genomes, very high quality *de novo* assembly of a genome is not uncommon overall. Nevertheless, the curation of even very well assembled MAGs is very rarely undertaken, perhaps due to the involvement of typically manual and generally not well understood steps. Here, we describe the methods that can be used for genome curation and provide examples to illustrate potential caveats along with their likely solutions. Our hope is that the following sections will motivate the development of new tools to enable routine curation of genomes from metagenomes.

A limited number of published complete metagenome-assembled genomes

To the best of our knowledge, as of 09/10/2019, 59 bacterial and three archaeal CMAGs from microbial community datasets are publicly available (**Table 1**). Of these, four CMAGs were finished using PacBio reads. The published CMAGs are primarily for members of the Candidate Phyla Radiation (CPR; 36 genomes) and DPANN (2 genomes), which have unusually small genomes (average genome size of 1.0 Mbp; Table 1). Other reported CMAGs include those for Proteobacteria (7 genomes), Saganbacteria (WOR-1; 4), Bacteroidetes (two), Candidatus Bipolaricaulota (two), Firmicutes (two), and one from each of Dependentiae (TM6; also small genomes), Elusimicrobia, Melainabacteria, Micrarchaeota, Nitrospirae, Zixibacteria and Candidatus Cloacimonetes (Table 1).

CMAGs are not limited to bacteria and archaea. Because all of the extracted DNA is sequenced, genomes are also reconstructed for phage and plasmids. In fact, the tool VirSorter (Roux et al. 2015) predicts circularized sequences suitable for verification and curation to remove gaps and local assembly errors. Two recent studies reported unusually large complete phage genomes. In the first case, 15 complete megaphage genomes, each > 540 kbp in length, were reconstructed and curated from human and animal microbiomes (Devoto et al. 2019). In the second case, 35 complete genomes > 200 kbp derived from phage, including the largest phage genomes yet reported (Al-Shayeb et al. 2019). The distinction of these sequences from prophage and the accurate size determinations could not be made without circularized genomes, and the complete, accurate inventory of genes would be precluded with only draft genomes.

Table 1. List of complete metagenome-assembled genomes. *The CMAG was reconstructed from a sample with only one organism present. [#]Wrongly labeled in NCBI as TM6. Note that many genomes exhibit asymmetric patterns of GC skew, which is attributed to uneven length replichores (also seen in isolate genome analysis). [$]Bidirectional skew patterns are not expected in many archaea. Grey shading indicates essentially identical genomes independently assembled from different samples. To date, CMAGs have been reconstructed for organisms from 30 different phylum-level groups. Five of the listed genomes are complete sequences were completed in the current study.

Taxonomy	Genome	Size (bp)	Genbank Accession	GC_skew	Reference
Archaea; DPANN; Diapherotrites	Candidatus Forterrea multitransposorum	839,632	CP045477	Archaeal bidirectional	Probst and Banfield (2018)
	archaeon GW2011_AR10	1,241,428	CP010424	Archaeal [$]	Castelle et al. (2015)
Archaea; DPANN; Micrarchaeota	ARMAN-2	1,007,044	ACVJ0000000	Archaeal bidirectional	Brett et al. (2010)
Bacteria; CPR; Roizmanbacteria	Candidatus Roizmanbacteria bacterium RIFOXYA2_FULL_38_14	1,216,931	MGBH01000001	As expected	Anantharaman et al. (2016)
	Candidatus Roizmanbacteria bacterium RIFOXYA1_FULL_37_12	1,216,931	MGBF01000001	As expected	Anantharaman et al. (2016)
	Candidatus Roizmanbacteria bacterium RIFOXYB1_FULL_37_23	1,216,931	MGBJ01000001	As expected	Anantharaman et al. (2016)
	Candidatus Roizmanbacteria bacterium RIFOXYC1_FULL_38_14	1,216,967	MGBN01000001	As expected	Anantharaman et al. (2016)
	Candidatus Roizmanbacteria bacterium RIFOXYD1_FULL_38_12	1,216,931	MGBR01000001	As expected	Anantharaman et al. (2016)
Bacteria; CPR; Peregrinibacteria	Candidatus Peribacter riflensis RIFOXYD2_FULL_PER-ii_58_23	1,248,180	CP013066	As expected	Anantharaman et al. (2016b)
	Candidatus Peribacter riflensis RIFOXYC2_FULL_PER-ii_58_32	1,248,112	CP013064	As expected	Anantharaman et al. (2016b)
	Candidatus Peribacter riflensis RIFOXYB2_FULL_PER-ii_58_17	1,248,181	CP013063	As expected	Anantharaman et al. (2016b)
	Candidatus Peribacter riflensis RIFOXYA2_FULL_PER-ii_58_14	1,248,026	CP013062	As expected	Anantharaman et al. (2016b)
Bacteria; CPR; Peregrinibacteria	BJP_IG2102_PER_44_74_curated	998,424	TBA	Rolling circle-like	this study
Bacteria; CPR; Collierbacteria	Candidatus Collierbacteria bacterium RIFOXYC2_FULL_45_15	1,089,434	MFAP01000001	Rolling circle-like	Anantharaman et al. (2016)
	Candidatus Collierbacteria bacterium RIFOXYD2_FULL_45_13	1,089,434	MFAS01000001	Rolling circle-like	Anantharaman et al. (2016)
	Candidatus Collierbacteria bacterium RIFOXYA2_FULL_46_20	1,089,434	MFAL01000001	Rolling circle-like	Anantharaman et al. (2016)
	Candidatus Collierbacteria bacterium RIFOXYB2_FULL_46_14	1,089,434	MFAN01000001	Rolling circle-like	Anantharaman et al. (2016)
Bacteria; CPR; Katanobacteria	candidate division WWE3 bacterium RIFOXYA1_FULL_40_11	897,158	MEVO01000001	As expected	Anantharaman et al. (2016)
	candidate division WWE3 bacterium RIFOXYB1_FULL_40_22	897,158	MEVU01000001	As expected	Anantharaman et al. (2016)
	candidate division WWE3 bacterium RIFOXYC1_FULL_40_10	897,158	MEWB01000001	As expected	Anantharaman et al. (2016)
Bacteria; CPR; Katanobacteria	Candidate division WWE3 bacterium RAAC2_WWE3_1	878,109	CP006914	Uncertain/uneven replicores	Kantor et al. (2013)
Bacteria; CPR; Azambacteria	Candidatus Azambacteria bacterium RIFOXYC1_FULL_42_20	585,024	MEYZ01000001	As expected	Anantharaman et al. (2016)
	Candidatus Azambacteria bacterium RIFOXYD1_FULL_42_38	585,024	MEZB01000001	As expected	Anantharaman et al. (2016)
Bacteria; CPR; KAZAN	candidate division Kazan bacterium RIFCSPHIGHO2_01_FULL_46_14	699,981	METB01000001	Uncertain/uneven replicores	Anantharaman et al. (2016)
	candidate division Kazan bacterium RIFCSPLOWO2_01_FULL_46_19	699,981	METD01000001	Uncertain/uneven replicores	Anantharaman et al. (2016)
Bacteria; CPR; KAZAN	candidate division Kazan bacterium GW2011_GWA1_50_15	602,646	CP011216	Uncertain/uneven replicores	Brown et al. (2015)
Bacteria; CPR; Saccharibacteria (TM7)	Candidatus Saccharimonas aalborgensis	1,013,781	CP005957	As expected	Albertsen et al. (2013)
	Candidatus Saccharibacteria bacterium GW2011_GWC2_44_17	1,038,683	CP011211	As expected	Brown et al. (2015)
	Candidatus Saccharibacteria bacterium YM_S32_TM7_50_20	1,450,269	CP025011	As expected	Starr et al. (2018)
	Candidatus Saccharibacteria bacterium RAAC3_TM7_1	845,464	CP006915	As expected	Kantor et al. (2013)
Bacteria; CPR; Dojkabacteria (WS6)	Candidatus Dojkabacteria bacterium HGW-Dojkabacteria-1	733,750	PHAO00000000	As expected	Hernsdorf et al. (2017)
	GWF2_GWF2_WS6_complete_39_15	896,362	TBA	As expected	this study
Bacteria; CPR; Absconditabacteria	Candidate division SR1 bacterium RAAC1_SR1_1	1,177,760	CP006913	Noisy, probably as expected	Kantor et al. (2013)
Bacteria; CPR; Beckwithbacteria	Candidatus Beckwithbacteria bacterium GW2011_GWC1_49_16	1,049,888	CP011210	No skew	Brown et al. (2015)
Bacteria; CPR; Berkelbacteria	Berkelbacteria bacterium GW2011_GWE1_39_12	915,059	CP011213	As expected	Brown et al. (2015)
	SR2-17_Biohub_180515_Berkelbacteria_Complete_circularized_51_91	768,550	TBA	As expected	this study
Bacteria; CPR; Pacebacteria	Candidatus Pacebacteria bacterium GW2011_OP11-3_36_13 [#]	853,053	SAMN03319330	As expected	Brown et al. (2015)
Bacteria; CPR; Parcubacteria (OD1)	Candidatus Parcubacteria ALT_46_28	1,133,667	TBA	As expected	this study
Bacteria; CPR; Campbellbacteria	Candidatus Campbellbacteria bacterium GW2011_OD1_34_28	752,630	CP011215	As expected	Brown et al. (2015)
Bacteria; CPR; Gracilibacteria (BD1-5)	BD02T64_BD1-5	1,343,103	SUB5359196	As expected	Sieber et al. (2019)
Bacteria; CPR; Kaiserbacteria	Candidatus Kaiserbacteria bacterium RIFCSPLOWO2_12_FULL_45_26	962,580	MFMM01000001	As expected	Anantharaman et al. (2016)
Bacteria; CPR; Woesebacteria	Candidatus Woesebacteria bacterium GW2011_GWF1_31_35	819,458	CP011214	As expected	Brown et al. (2015)
Bacteria; CPR; Wolfebacteria	Candidatus Wolfebacteria bacterium GW2011_GWB1_47_1	984,447	CP011209	As expected	Brown et al. (2015)
Bacteria; Bacteroidetes	Candidatus Fluviicola riflensis	4,551,443	CP022585	As expected	Banfield at al. (2017)
	Bacteroidetes UKL13-3	3,236,529	CP012155	As expected	Driscoll et al. (2017)
Bacteria; Candidatus Bipolaricaulota	Candidatus Acetothermia bacterium Ran1	1,324,338	LS483254	Uncertain/low skew	Hao et al. (2018)
	Candidatus Bipolaricaulis sp. Ch78	1,701,655	CP034928	As expected	Kadnikov et al. (2019)
Bacteria: Candidatus Cloacimonetes (WWE1)	Candidatus Cloacamonas Acidaminovorans (via fosmid library)	2,246,820	NC_020449.1	As expected	Pelletier et al. (2008)
Bacteria; Candidatus Zixibacteria	Candidate division Zixibacteria bacterium RBG-1	2,122,767	AUYT01000001	As expected	Castelle et al. (2013)
Bacteria; Elusimicrobia	Candidate phylum Termite Group 1 Rs-D17	1,125,857	NC_020419	As expected	Hongoh et al. (2008)
Bacteria; Firmicutes	Candidatus Desulforudis audaxviator *	2,349,476	NC_010424	As expected	Chivian et al. (2008)
	Bacterium AB1 isolate AB1	593,366	CP017117	Generally as expected	Miller et al. (2016)
Bacteria; Melainabacteria	Candidatus Melainabacteria bacterium MELA1	1,867,336	CP017245	As expected	Di Rienzi et al. (2013)
Bacteria; Nitrospirae	Nitrospira inopinata	3,295,117	NZ_LN885086	As expected	Daims et al. (2015)
Bacteria; Proteobacteria	Candidatus Liberibacter asiaticus str. Psy62 *	1,227,204	CP001677.5	As expected	Duan et al. (2009)
	SCNpilot_BF_INOC_Rickettsiales_complete_39_4	988,358	TBA	As expected	this study
	Ca. Riegeria santandreae (contain ambigous bases)	1,342,908	LR026963	Low skew / uncertain	Jäckle et al. (2019)
	Hyphomonadaceae UKL13-1	3,501,508	CP012156	As expected	Driscoll et al. (2017)
	EPL_02132018_0.5m_Candidatus_Fonsibacter_30_26	1,136,868	PRJNA552483	As expected	Chen et al. (2019)
	Betaproteobacterium UKL13-2	3,387,087	CP012157	As expected	Driscoll et al. (2017)
	Candidatus Pseudomonas sp. strain JKJ-1	6,408,606	PRJNA320198	*No genome available*	White et al. (2016)
	Candidatus Sulfuricurvum sp. RIFRC-1	2,358,861	CP003920	As expected	Handley et al. (2014)
Bacteria; Dependentiae (TM6)	candidate division TM6 bacterium *TM6SC1*	1,088,795	—	As expected	Antipov et al. (2016)
Bacteria; WOR-1	candidate division WOR-1 bacterium RIFOXYA12_FULL_52_29	1,668,697	METT01000001	As expected	Anantharaman et al. (2016)
	candidate division WOR-1 bacterium RIFOXYA2_FULL_52_19	1,668,697	METY01000001	As expected	Anantharaman et al. (2016)
	candidate division WOR-1 bacterium RIFOXYB2_FULL_52_9	1,668,697	MEUD01000001	As expected	Anantharaman et al. (2016)
	candidate division WOR-1 bacterium RIFOXYC12_FULL_52_18	1,668,697	MEUG01000001	As expected	Anantharaman et al. (2016)

Genome curation: filling scaffolding gaps and removal of local assembly errors

Genome curation requires the identification and correction of local assembly errors and removal of gaps at scaffolding points. However, the exclusion of these steps in current genome-resolved metagenomics studies propagate errors such as incomplete or incorrect protein-coding gene sequences in public databases.

Automatic tools like Gapfiller (Nadalin et al. 2012) may be useful for the filling of 'N' gaps at scaffold joins (read pairs should span the gap if the scaffolding was done correctly). Our primary approach to gap filling makes use of unplaced pairs for reads adjacent to the gaps. When reads are mapped to genome fragments that comprise a bin, a file of unplaced paired reads is generated for each fragment. By mapping these unplaced paired reads to the corresponding fragment, it is usually possible to incrementally close the gap (so long as there is sufficient depth of coverage). After the first round of mapping of unplaced paired reads, the consensus

364 sequence must be extended into the gap before remaining unplaced paired reads are remapped. The newly
365 introduced paired reads should be placed at an appropriate distance from their existing pairs, given the
366 fragment insert size. Often a few iterations are needed for gap closure. However, if the gap does not close and
367 no further extension can be accomplished using the existing collection of unplaced pairs, the full metagenomic
368 read dataset can be mapped to the new version of the scaffold and another round of extension performed until
369 the gap is closed.
370 If a gap cannot be closed using the unplaced paired reads due to low coverage, one solution may be
371 to include reads from another sample in which the same population occurs (this may not be appropriate for
372 some investigations), or by performing a deeper sequencing of the same sample. In other cases, the necessary
373 reads are misplaced, either elsewhere on that scaffold or on another scaffold in the bin. This happens because
374 the reads have been "stolen" thus the true location sequence is not available to be mapped to. This often leads
375 to read pileups with anomalously high frequencies of SNVs in a subset of reads. However, anomalously high
376 read depths can also occur due to mapping of reads from another genome. The misplaced reads can be located
377 based on read names and extracted for gap filling. Other indications of misplacement of reads include read
378 pairs that point outwards (rather than towards each other, as expected) or with unusually long paired read
379 distances. One of these reads is misplaced and the other read normally constrains the region to which the pair
380 must be relocated. Relocation of the misplaced read can often lead to filling of scaffolding gaps. In some cases,
381 gap filling cannot be easily achieved despite sufficient read depth. This can occur, for example, due to complex
382 repeats. Sometimes these repeat regions can be resolved by careful read-by-read analysis, often requiring
383 relocation of reads based on the placement of their pairs as well as sequence identity.
384 Another important curation step is the removal of local assembly errors (Figure S3). We suspect that
385 these errors are particularly prominent in IDBA_UD assemblies, although it is likely that all assemblers
386 occasionally make local assembly errors. Local assembly errors can be identified because the sequence in that
387 region lacks perfect support, by even one read. The region should be opened up and each read within that
388 region separated to the appropriate side of the new gap (so that all reads match the consensus sequence).
389 Unsupported consensus sequence should be replaced by Ns. The new gap can be filled using the procedure for
390 filling scaffolding gaps, as described above.
391 A second type of local assembly error is where 'N's have been inserted during scaffolding despite
392 overlap between the flanking sequences (Figure S4). We have observed this problem with both IDBA_UD and
393 CLC workbench assemblies. The solution is simply to identify the problem and close the gap, eliminating the Ns
394 and the duplicate sequence.
395 Another common assembly error involves local repeat regions in which an incorrect number of
396 repeats has been incorporated into the scaffold sequence. This situation may be detected by manual inspection
397 of read mapping profile, as it leads to anomalous read depth over that region. Sometimes the correct number
398 of reads may only be approximated based on the consistency of the coverage within the repeat region and
399 other parts of the scaffold (see example below).
400 Rarely, in our experience, assemblers create scaffolds that are chimeras of sequences from two
401 different organisms (e.g., (Rojas-Carulla et al. 2019)). These joins typically lack paired read support and/or can
402 be identified by very different coverage values and/or phylogenetic profiles on either side of the join.
403 Another seemingly rare error involves the artificial concatenation of an identical sequence,
404 sometimes of hundreds of bp in length, repeated up to (or more than) three times. This has been a problem
405 with some sequences of seemingly large phage deposited in public databases (as discussed by Devoto et al.
406 2019 and Al-Shayeb, Sachdeva et al. 2019). This phenomenon is easily identified by running a repeat finder, a
407 step that should also be included in the curation to completion pipeline (see below).
408
409 **From high quality draft sequences to complete genomes from metagenomes**
410 Genome curation to completion is rarely undertaken (Table 1) because there is no single tool available to
411 accomplish it, and there can be confusing complications. The procedure requires the steps described in the
412 prior section as well as extension of scaffolds (or contigs, if no scaffolding step was undertaken) so that they
413 can be joined, ultimately into a single sequence (assuming the genome is a single chromosome). With currently

414 available tools, this is time consuming, sometimes frustrating and often does not result in a CMAG (usually
415 because of indistinguishable multiple options for scaffold joins typically due to repeats such as identical copies
416 of transposons). However, when it can be done, the resulting genome solution should be essentially unique, as
417 we will show below. There is nothing 'arbitrary' about the process, except occasionally the choice of which set
418 (usually a pair) of sub-equal locus variants (e.g., SNVs) will represent the final genome. Even in those cases,
419 depending on the availability of multiple appropriate metagenomes for read recruitment analyses, tools for
420 haplotype deconvolution such as DESMAN (Quince et al. 2017) may offer quantitative support for such
421 decisions.
422 In our experience, the most important first step in the path toward recovery of a CMAG is to start
423 from a well-defined bin that appears to comprise the vast majority of the genome of interest (step 1; Figure 4).
424 As above, this is usually determined based on genome completeness evaluation (step 2; Figure 4) and/or a very
425 strong set of binning signals (see Figure S1 for example). It should be noted that some genomes (e.g., CPR
426 bacteria) may naturally lack certain SCGs that are otherwise considered universal in other bacteria (Brown et al.
427 2015), and may require a modified list of universal SCGs such as those proposed for CPR genomes for more
428 accurate evaluations of completion (Anantharaman et al. 2016). Importantly, the targeted bin should be
429 polished to remove contamination scaffolds, as noted above (step 3; Figure 4).
430 Given currently available tools, it is probably wise to choose a bin with no more than 10 pieces (step
431 4; Figure 4), although a MAG with larger number of scaffolds can be curated to completion if necessary (Chen
432 et al. 2019). The best possible case is when the genome is *de novo* assembled into a single piece. In some cases,
433 the genome is already circularized, based on overlap sequences at the scaffold ends, with paired-end reads
434 that span the scaffold ends. Although rare, this does occur, mostly for small genomes (e.g., Saccharibacteria;
435 Albertsen et al. 2013; Starr et al. 2018). In other cases, a modest amount of end extension may be required for
436 circularization (see below). The single scaffold should be checked for complete coverage and support of the
437 consensus. Gaps or local assembly errors must be dealt with before the genome is classified as curated and
438 complete (some additional checks are described below).
439 Some assemblers (e.g., IDBA_UD, metaSPAdes) retain sequences that are non-unique at scaffold
440 ends. Assembly termination presumably happens because assembly algorithms are designed to stop at points
441 of uncertainty rather than risk making incorrect joins (Figure S5A). Incidentally, as different assemblers can
442 yield different results, there can be value in comparing the results for the same data assembled using different
443 tools and/or parameters (see examples below). Also, in some cases, assembly of scaffolds representing the
444 same organism (or a closely related organism) from a related sample, could help scaffold extension and/or
445 linkage (Figure S5B). Potential scaffold joins can be made by identifying perfect overlaps at the ends of
446 scaffolds of a MAG ("overlap-based assembly", Step 5; Figure 4). Often, the length of perfect overlap of
447 scaffolds assembled using IDBA_UD and metaSPAdes is n-1 or n, respectively, where n is the largest k-mer size
448 used in *de novo* assembly. Although the assembler chose not to make these joins (possibly due to confusion
449 involving even a single read), seemingly unique joins involving scaffolds in a bin can be made tentatively during
450 curation. Ultimately, non-unique joins can be eliminated or resolved at the end of the curation process. It is
451 important to note that non-uniqueness of a join may not be evident in an initial scaffold set due to failure to
452 include a relevant scaffold in the bin or lack of *de novo* assembly of relevant regions. Thus, it is important to
453 test for repeated regions that cannot be spanned by paired reads at the end of curation (either in the
454 potentially complete genome or curated scaffold set if completion is not achieved). Failure to identify perfect
455 repeats can also lead to problems in isolate genomes, as we show below.
456 Scaffolds within a bin that do not overlap at the start of curation may be joined after one or more
457 rounds of scaffold extension (Figure S6). This process of extending, joining and remapping may continue until
458 all fragments comprise a single circularized sequence. It should be noted that read by read scaffold extension is
459 very time consuming. If an extended scaffold cannot be joined to another scaffold after a few rounds of
460 extension it may be worth testing for an additional scaffold (possibly small, thus easily missed by binning) by
461 searching the full metagenome for overlaps (steps 6 and 7, Figure 4). Sometimes, the failure of scaffold
462 extension is due to missing paired reads, which may be found at the end of another fragment. If they are
463 pointing out but the sequences cannot be joined based on end overlap, a scaffolding gap can be inserted in the

464 joined sequence (reverse complementing one of the scaffolds may be necessary). Closure of the new
465 scaffolding gap uses the approach described above.
466 During the attempt to obtain a circularized sequence, it is important to note that if the genome has
467 a single pair of duplicated sequences that are larger than can be spanned by paired reads, a reasonable
468 solution can be found if the genome bin is curated into just two pieces. In this case, the only solutions are
469 either resolution into two chromosomes or generation of a single genome (Figure S7). This observation
470 underlines the importance of curation from a high quality bin, as curation from a full metagenome would leave
471 open the existence of other scaffolds that also bear that repeat.
472 Once the genome is circularized, it is important to check for repeats larger than spanned by paired-
473 end reads (as noted above; step 8, Figure 4). Assuming a seemingly CMAG is achieved, several steps to further
474 verify the accuracy of the assembly path may be warranted (step 9, Figure 4). First, reads may be mapped to
475 the sequence allowing no mismatches to confirm no coverage gaps due to base miscalls and to verify that no
476 region has abnormal coverage. Tools that provide interactive visualization and inspection of coverage patterns,
477 such as anvi'o, Geneious (Kearse et al. 2012) or 'Integrative Genomics Viewer' (Robinson et al. 2011), may be
478 used for this task. Second, we advocate verification of paired read placements over the entire assembly to
479 check for problem areas that may have been missed in automated procedures. Abnormally low coverage may
480 be due to a subpopulation variant, whereas higher than expected coverage could indicate the existence of a
481 block of sequence that was pinched out from the genome at a repeated region. Systematic decline of coverage
482 from origin to terminus of replication is expected if genome replication was ongoing at the time of sampling
483 (see below). Third, the presence of expected genes (e.g., universal SCGs) should be verified. The genome can
484 be classified using phylogenetic analyses (e.g., based on 16S rRNA gene or concatenated ribosomal proteins
485 sequences; step 10, Figure 4). After the completion of MAG, the start of the genome should be moved to the
486 non-coding region near the origin of replication (steps 11 and 12, Figure 4). See below for details regarding how
487 GC skew can be used to locate the origin.
488 An important consideration in genome curation to completion is knowing when to give up. In some
489 cases, failure to circularize after a few rounds of curation may be an indication that the effort could be better
490 invested in other activities. If alternative assembly paths that cannot be distinguished by the unique placement
491 of paired reads are identified, failure may be on the horizon. However, as noted above (Figure S7), it can be
492 appropriate to continue curation as a final unique solution may be possible even in the presence of a repeat
493 that cannot be spanned by paired reads.

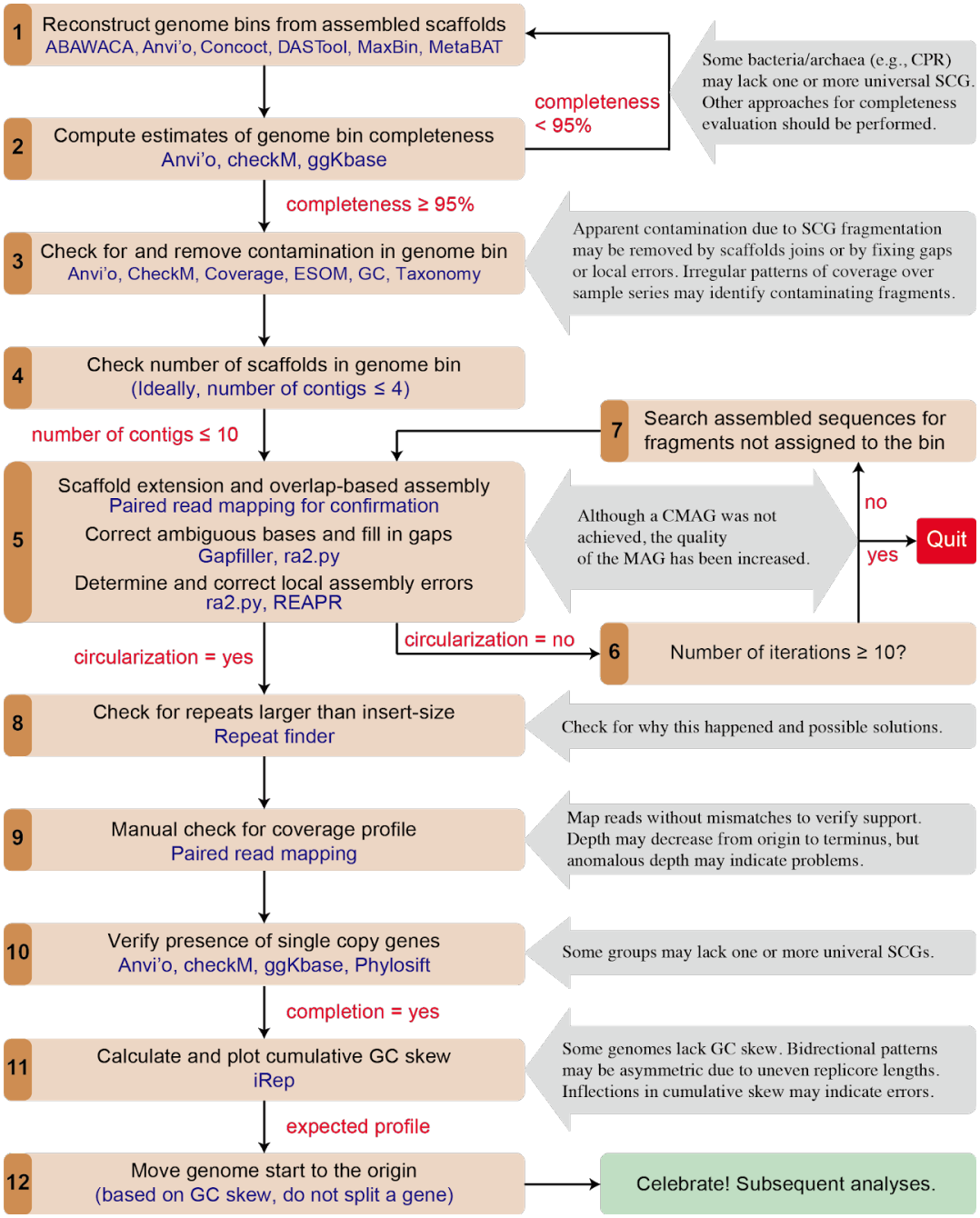

Figure 4. The workflow for generating curated and complete genomes from metagenomes. Steps are shown in black font and the tools or information used in blue font. Notes for procedures are shown in gray boxes.

Case studies illustrating the curation of draft MAGs

Here we illustrate how a draft MAG can be curated to completion or into better quality status, with step-by-step procedures detailed in the Supplementary Information.

Case one, curation of a CPR genome to completion. ALT_04162018_0_2um_scaffold_13, length of 1,128,909 bp, was the only scaffold in the binned MAG (i.e., bin.56) from MetaBAT (Figure S8). CheckM reported 70.1% completeness without contamination, and preliminary analyses based on 16S rRNA and rpS3 genes identified it as a Parcubacteria genome. This genome was likely near complete based on the detection of all CPR universal SCGs, though we did not identify overlap at the ends of the scaffold that would circularize it. This scaffold could

508 be circularized after a single round of scaffold end extension, with read pairs placed at the ends of the scaffold.
509 In fact, we found two very small assembled sequences that were variants of each other and both could be used
510 for circularization. The non-uniqueness of this region terminated the original assembly. We chose the dominant
511 variant to represent the population genome. No repeat sequence longer than the sequencing insert size was
512 detected. A total of 13 local assembly errors were reported by ra2.py. All these errors were manually fixed and
513 validated, including a complicated error in the sequence of a protein-coding gene that contains multiple repeat
514 regions. The complete genome has a length of 1,133,667 bp, and encodes 1,147 protein-coding genes, 47 tRNA
515 and a copy each of 5S/16S/23S rRNA genes.
516
517 *Case two, curation of a Betaproteobacteria genome without completion.* Bin.19 contained seven scaffolds (3.6
518 Mbp in size), and was evaluated by CheckM to be 98.42% complete with 0.12% contamination (Figure S9).
519 Analyses of the 16S rRNA gene sequence indicated it was a Betaproteobacteria (92% similarity to that of
520 *Sulfuricella denitrificans* skB26). After the first round of scaffold extension and assembly, only two scaffolds
521 could be combined (i.e., scaffold 21 and 25). We searched for the pieces that could be used to link the scaffolds
522 together using the newly extended parts of the scaffolds via BLASTn against the whole scaffold set. This
523 approach retrieved four short (584-1191 bp in length) and one longer piece (15,678 bp in length) that encodes
524 several bacterial universal SCGs including rpS7, rpS12, rpL7/L12, rpL10, rpL1 and rpL11 (which were absent
525 from bin.19), and whose two ends both encode elongation factor Tu (EF-Tu). Two of the four short pieces could
526 be perfectly joined in two possible places to the original scaffold set. Based on comparison with the *Sulfuricella*
527 *denitrificans* skB26 genome, we hypothesized the linkage patterns for these fragments and then considered the
528 two choices for how the resulting two large genome fragments could be arrayed. The linkage choices were
529 supported based on the overall pattern of GC skew (see below and Figure S9). Technically, however, the bin
530 remains as two contigs with two internal joins unsupported by unique paired read placement. Based on the GC
531 skew of the pair of contigs linked by Ns, the genome is near complete. After the fixation of local assembly
532 errors, it has a total length of 3.72 Mbp, encodes 3,544 protein-coding genes, 41 tRNA and one copy of each of
533 the 5S/16S/23S rRNA genes, and is clearly of higher quality than the original bin due to scaffold extension and
534 correction of local assembly errors.
535
536 *Case three, curation of a published incomplete genome to completion.* Here we completed a published curated
537 (for local assembly errors) but incomplete genome belonging to the order *Rickettsiales* (Kantor et al. 2017).
538 This genome was assembled *de novo* into a single circularizable 988 kbp scaffold, with two closely spaced gaps
539 (Figure S10a). Closing of these gaps required relocation of unplaced paired reads (Figures S10b and c).
540
541 In addition to the above-mentioned case studies, we curated three additional bacterial genomes to completion
542 as part of our methods refinement. These genomes are listed in **Table 1**.
543
544 **Using GC skew as a metric for checking genome correctness**
545 GC skew is a form of compositional bias (imbalance of guanosine (G) relative to cytosine (C) on a DNA strand)
546 that is an inherent feature of many microbial genomes, although some are known to display little or no GC
547 skew (e.g., certain Cyanobacteria, (Nakamura 2002)). The phenomenon of strand-specific composition was
548 described by Lobry (Lobry 1996), who observed that the relative GC skew changes the sign crossing the *oriC*
549 and *terC* regions. Thus, the inflection point in genome GC skew at the origin of replication is often close to the
550 dnaA gene and typically contains a small repeat array. GC skew is calculated as (G-C/G+C) for a sliding window
551 along the entire length of the genome (suggested window=1000 bp, slide=10 bp). The skew is also often
552 summed along the sequence to calculate cumulative GC skew. This was proposed by Grigoriev (Grigoriev 1998),
553 who showed that the calculation of the cumulative GC skew over sequential windows is an effective way to
554 visualize the location of the origin and terminus of replication. For complete genomes, the GC skew is often
555 presented starting at the origin of replication, proceeding through the terminus and back to the origin (i.e., as if
556 the chromosome was linear). The pattern of the cumulative GC skew, where the function peaks at the terminus
557 of replication, indicates that the genome undergoes bidirectional replication. The pattern is fairly symmetrical

558 unless the replichores are of uneven lengths. Because the magnitude of the cumulative GC skew varies from
559 genome to genome, the magnitude of the skew could potentially be used as a binning signal.
560 The explanation for the origin of GC skew is not fully agreed upon. It may arise in large part due to
561 differential mutation rates on the leading and lagging strands of DNA. Enrichment in G over C occurs due to C
562 deamination to thymine (C->T), the rates of which can increase at least 100-fold when the DNA is in a single
563 stranded state. In the process of DNA replication, the leading strand remains single stranded while the paired
564 bases are incorporated by the DNA polymerase into its complementary strand. However, the Okazaki
565 fragments on the lagging strand protect a fraction of the DNA from deamination. Thus, the leading strand
566 becomes enriched in G relative to C compared to the lagging strand. The magnitude of the GC skew can be
567 impacted by the speed of the DNA polymerase processivity (which impacts the length of time that the DNA is
568 single stranded) and the length of the Okazaki fragments. GC skew has been linked to strand coding bias (Rocha
569 et al. 1999). Concentration of genes on the leading strand would afford protection against non-synonymous
570 mutations (as C->T mutations in the wobble position of codons are always synonymous), whereas G->A on the
571 lagging strand (following C->T on the leading strand) in two cases results in nonsynonymous mutations (AUA
572 for Ile vs. AUG for Met, and UGA for stop codon vs. UGG for Trp). The potential for deamination in the non-
573 coding strand during transcription, another source of GC skew, would also favor genes on the leading strand.
574 GC skew persists because the leading strand is maintained as such through subsequent replication events.
575 Given that a well-defined pattern of GC skew is anticipated across many bacterial (and some
576 archaeal) genomes, we wondered whether plots of cumulative GC skew for putative complete genomes can be
577 confidently used to test for genome assembly errors. For this metric to be useful, it would be imperative to
578 establish the extent to which GC skew is indeed a feature of complete bacterial genomes. To our knowledge,
579 the now extensive set of complete isolate genomes has not been leveraged to do this.
580 We undertook benchmarking of GC skew, and more specifically cumulative GC skew, using all ~7000
581 complete genomes in the RefSeq database. We found that the majority of RefSeq bacterial genomes show the
582 expected pattern of cumulative GC skew. Interestingly, the magnitude of the origin to terminus skew varies
583 substantially, from ± 0.4 excess G relative to C to close to zero (Figure S11). A small subset of the ~7000
584 complete genomes essentially lack GC skew (as reported for some Cyanobacteria, see above) (Table S6). Poorly
585 defined (noisy) patterns are often associated with low total cumulative skew. About 15% of genomes have
586 notably asymmetric patterns (i.e., the cumulative skew is substantially larger for one half of the chromosome
587 relative to the other), presumably because the two replichores are of substantially uneven length. Moreover,
588 some bacterial genomes had a GC skew pattern indicating rolling circle replication (Table S7). Interestingly, we
589 did not detect a strong correlation between the magnitude of GC skew and bias for genes on the leading
590 strand.
591 Some complete genomes have quite aberrant skew patterns, with inversions in the cumulative skew
592 within a single replichore or exceedingly uneven predicted replichore lengths. We considered the possibility
593 that a subset of these isolate genomes may contain mis-assemblies. Such a phenomenon was already shown by
594 Olm et al. in the case of a *Citrobacter koseri* isolate genome that was clearly wrongly assembled across rRNA
595 operons (and a PacBio assembly for a closely related strain showed the expected pattern of cumulative GC
596 skew) (Olm et al. 2017). To test for the possibility that these other complete genomes contained errors, we
597 posited that mis-assemblies would likely occur at perfect repeats that are longer than the distance spanned by
598 paired reads. Further, we predicted that the pair of repeats flanking the wrongly assembled sequence region
599 would be in reverse complement orientations so that the intervening DNA segment could be flipped at the
600 repeats and that the flipped version would exhibit the expected GC skew pattern. In five of twelve cases that
601 we scrutinized it was possible to show that reverse complementing the sequence spanned by repeats indeed
602 resulted in genomes with exactly the expected form of cumulative GC skew (Figures 5, S12 and S13). In one
603 case, i.e., *Flavobacterium johnsoniae* UW101 (NC_009441.1), the original assembly notes indicated assembly
604 uncertainty (although the complete genome was deposited at NCBI).
605 We acknowledge the possibility that a recent major rearrangement could also give rise to inflexions
606 in GC skew, however major rearrangements typically have a well-defined placement relative to the origin of
607 replication that is inconsistent with the patterns observed (Eisen et al. 2000). Although we cannot state that

these isolate genomes are wrongly assembled, we suggest that it is a distinct possibility. Incorrect assemblies in isolate genomes can be of high significance, given the trust placed in them for evolutionary and metabolic analyses that make use of synteny and gene context. They are also used as references for calculation of growth rates via the PTR method (Korem et al. 2015), and incorrect reference sequences will corrupt such measurements.

It is well known that some archaea replicate their genomes from multiple origins (Barry and Bell 2006). In such cases, the cumulative GC skew pattern is not a useful test of overall genome accuracy. However, some archaea do show the peaked pattern that is typical of bacteria, thus indicative of bidirectional replication. Overall, we found 18 of 224 RefSeq archaeal genomes tested that show this pattern, and all of them are Euryarchaeota (Table S8). In addition, this pattern was reported for a DPANN archaeon (Probst and Banfield 2018).

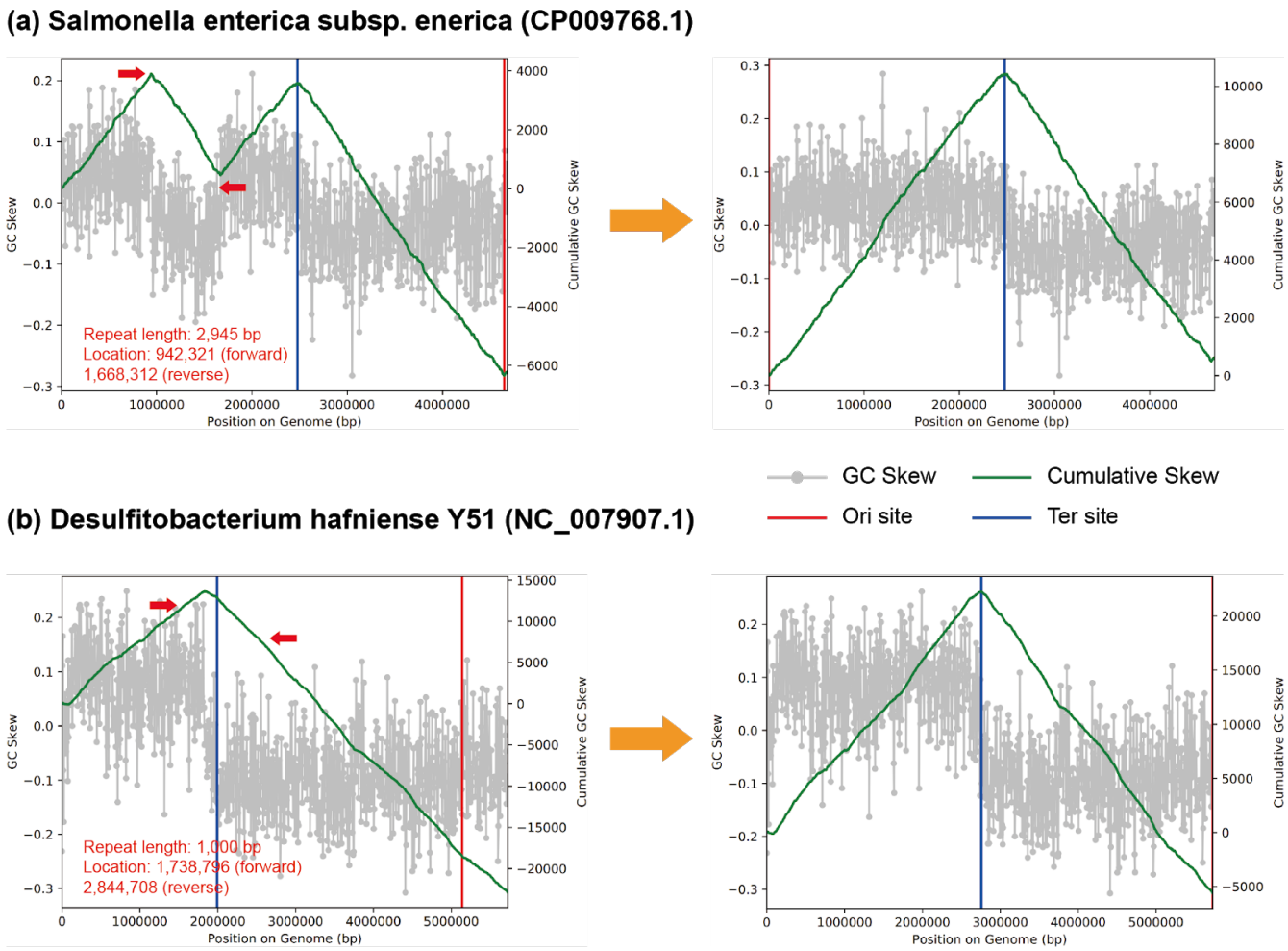

Figure 5. Examples of probable assembly errors in RefSeq bacterial genomes. The diagrams show the GC skew (grey) and cumulative GC skew (green line) of the original (left) and the modified (right) versions of the genomes (all calculated with window size of 1000 bp, and slide size of 10 bp). The location and direction of repeat sequences leading to the abnormal GC skew are indicated by red arrows. After flipping the repeat-bounded sequences the genomes show the pattern expected for genomes that undergo bidirectional replication (right). For more examples, see Figures S12 and S13.

Other approaches, future opportunities and challenges

Single-cell genomics. Microbial single-cell sequencing is a family of strategies that typically use microfluidics and whole-genome amplification to physically isolate individual cells and sequence their genomes without

632 cultivation (Stepanauskas 2012). The resulting single-amplified genomes (SAGs) can offer critical insights into
633 microbial lifestyles (Swan et al. 2011), and shed light on intra-population structures of complex microbial
634 consortia (Kashtan et al. 2014) or naturally occurring host-virus interactions (Labonté et al. 2015), where short-
635 read and assembly-based strategies may not be effective. However, state-of-the-art single-cell sequencing
636 strategies typically generate highly fragmented and incomplete genomes due to the need for random
637 amplification arising from small quantities of DNA present in a single cell (Kalisky and Quake 2011). In some
638 cases, sequences from other organisms may contaminate individual wells (Rinke et al. 2013), in other cases
639 combining sequences from different cells into single draft genomes based on sequence identity thresholds of
640 phylogenetic markers (i.e. > 97% 16S rRNA identity; (Rinke et al. 2013)), may result in hybrid genomes. In fact
641 these hybrids are potentially from different species, given that many consider 97.9% 16S rRNA sequence
642 divergence as a proxy for the species boundary (Newton et al. 2007; Garcia et al. 2018). Interestingly, Probst et
643 al. indicate that although the cells are often chosen for single cell sequencing based on their amplified 16S
644 rRNA genes, the sequences recovered do not always match the amplified genes (Probst et al. 2018). Some of
645 these problems may be ameliorated with additional steps of binning and refinement, and similar to MAGs,
646 SAGs can also be curated to completion as demonstrated by at least one study that used long (Sanger) reads in
647 conjunction with short read assemblies (Woyke et al. 2010). Given the fast pace of improvements in
648 microfluidics technologies as well as whole-genome amplification and sequencing chemistry (Woyke et al.
649 2017), we anticipate that single-cell genomics will continue to gain popularity and its joint use with other
650 genome-resolved metagenomics strategies will become increasingly frequent.
651
652 ***Complete genomes from long-reads.*** Among the published CMAGs, four were obtained by assembly of PacBio
653 reads, including three proteobacterial and one Bacteroidetes genome (White et al. 2016; Driscoll et al. 2017).
654 Especially Oxford Nanopore Technologies offers affordable, easy-to-operate, and portable sequencers for long-
655 read sequencing. While improving, errors from nanopore sequencing can dramatically exceed state-of-the-art
656 short read sequencing (Laver et al. 2015), however, new approaches for long-read correction (Rang et al. 2018;
657 Arumugam et al. 2019), hybrid assembly (Wick et al. 2017), and mock community standards (Nicholls et al.
658 2019) are emerging. Short read-based assembly strategies often report fragmented contigs due to repeat
659 elements that exceed short read lengths, which is an issue long-read sequencing overcomes, improving the
660 quality of genomes from metagenomics (Arumugam et al. 2019). We anticipate that the combination of short
661 reads and long-reads sequencing will be an increasingly common strategy for recovery of highly curated and
662 complete genomes from microbial community samples.
663
664 ***Chromosome conformation capture method***. The chromosome conformation capture (i.e., 3C) is a method
665 that enables the determination of physical contacts between different regions of a chromosome and between
666 the different chromosomes of a cell (Dekker et al. 2002). The initial applications of this strategy focused on
667 eukaryotic genomes and revealed, for example, the folding principles (Lieberman-Aiden et al. 2009) and the
668 chromatin looping (Rao et al. 2014) of the human genome. The 3C approach has recently been developed into
669 multiple derivative proximity ligation methods such as Hi-C (Lieberman-Aiden et al. 2009) and meta3C
670 (Marbouty et al. 2014), and applied to individual microbial populations (Le et al. 2013) as well as complex
671 assemblages of environmental microbes (Marbouty et al. 2014). As these approaches offer physical linkage
672 between DNA fragments that are proximal to each other, they can improve metagenomic binning (Baudry et al.
673 2019; DeMaere and Darling 2019). While promising, the additional complexity of library preparations and
674 additional cost due to the need for separate metagenomic libraries (Liu and Darling 2015) prevent their routine
675 application to metagenomic studies. In addition, distinct populations that are in close proximity in the input
676 sample and repeat sequences may yield misleading contact signals and result in chimeric assemblies (Marbouty
677 and Koszul 2015). Nevertheless, the application of proximity ligation strategies to naturally occurring complex
678 microbial consortia can provide important insights (Bickhart et al. 2019; Stalder et al. 2019).
679
680 ***Eukaryotes and even macroorganisms.*** The assembly of draft eukaryotic genomes from shotgun metagenomes
681 is possible, despite the large genome sizes of most eukaryotes. However, eukaryotic MAGs can be readily

682 contaminated by fragments of genomes from coexisting bacteria and archaea (Boothby et al. 2015; Arakawa
683 2016), so careful evaluation is needed to avoid misleading conclusions (Delmont and Eren 2016). We have
684 found that phylogenetic profiling of contigs based on best matches in reference databases can be an effective
685 way to identify contaminating bacterial and archaeal sequences.
686 An important step for recovery of reasonable quality eukaryotic genomes from metagenomes is to
687 separate assembled eukaryotic from prokaryotic genome fragments prior to binning. Then, eukaryote-specific
688 gene predictions can be established and gene annotations used to estimate genome completeness. The K-mer-
689 based classifier, EukRep, was developed to accomplish this separation (West et al. 2018). Although eukaryote
690 genome recovery from metagenomes is increasingly reported (Quandt et al. 2015; Mosier et al. 2016; Olm et
691 al. 2019), to our knowledge, none have been extensively curated or completed.
692
693 ***High fragmentation of metagenomic scaffolds.*** A major limitation on the quality of MAGs relates to genome
694 fragmentation. Fragmentation is doubly problematic because small fragments are hard to bin accurately and
695 gaps result in incomplete gene inventories. Fragmentation can arise due to the presence of duplicated
696 sequences (e.g., transposases, rRNA operons), but the most pronounced problems usually are the result of
697 coexisting closely related strains that confuse de Bruijn graph based assemblers (Olson et al. 2017). For
698 example, although *Prochlorococcus* and SAR11 are among the most abundant bacteria in ocean habitats, the
699 co-occurence of closely related strains (Giovannoni 2017) leads to very fragmented MAGs and poor
700 representation in the final datasets (Delmont et al. 2018; Tully et al. 2018). Of the three commonly used
701 metagenomic assemblers, IDBA_UD, MEGAHIT, metaSPAdes (Greenwald et al. 2017), metaSPAdes was best
702 designed to handle micro-variations between fragments from related strains to generate longer composite
703 sequences (Olson et al. 2017). However, care should be taken when undertaking detailed analyses (e.g.,
704 biochemical testing) of open reading frames generated in this way as they may be chimeric.
705 Practically, another approach that can sometimes address the problem of assembly fragmentation
706 due to strain variety is collections of sequences from related samples (e.g., along a geochemical gradient) to
707 identify communities in which there is much reduced complexity of related strains. For example, opportunities
708 can arise due to the recent proliferation of one strain over the background of numerous closely related strains
709 following changes in environmental conditions. In other words, if a genome cannot be recovered from one
710 sample, look for it in related samples. We anticipate that this approach will be most effective for genome
711 recovery from soil environments, where strain diversity can be extreme and environmental heterogeneity
712 provides access to different strain mixtures.
713
714 **Conclusions**
715 Genomes derived from metagenomes have advanced our understanding of microbial diversity (Hug et al. 2016;
716 Anantharaman et al. 2016; Parks et al. 2017) and metabolism (e.g., (van Kessel et al. 2015; Anantharaman et al.
717 2018). However, these genomes are readily adopted by the scientific community for a wide variety of
718 investigations, and errors will propagate. In fact, the proposal of a new nomenclature for large swaths of the
719 tree of life based largely on MAGs (Parks et al. 2018) brings a potential crisis into focus. We conclude that it is
720 imperative that complete, curated genomes are recovered for all major lineages (including those that lack any
721 isolated representative). The increased span of phylogenetic coverage by complete genomes will provide a
722 valuable reference set against which newly recovered genomes can be confidently compared and augment
723 what has been achieved by the isolate-based Genome Encyclopedia of Bacteria and Archaea program (Wu et
724 al. 2009). New complete sequences from previously genomically undescribed lineages will also improve
725 understanding of how protein families and functions are distributed, facilitate more powerful analyses of
726 evolutionary processes such as lateral gene transfer and enable more accurate phylogenetic representations of
727 life's diversity. Finally, we advocate for the development of methods to routinely curate assemblies and draft
728 genomes (if not to completion) at scale to ensure the accuracy of evolutionary and ecosystem insights.
729
730 **Methods**
731 **Preparation of MAGs as examples for genome curation**

732 This study includes two MAGs were not previously published, as examples for genome curation. These
733 genomes were assembled from samples collected in a mine tailings impoundment (Manitoba, Canada). The
734 raw reads of metagenomic sequencing were filtered to remove Illumina adapters, PhiX and other Illumina trace
735 contaminants with BBTools (Bushnell 2018), and low-quality bases and reads using Sickle (version 1.33;
736 https.github.com/najoshi/sickle). The high-quality reads were assembled using both IDBA_UD (Peng et al.
737 2012) and metaSPades (Nurk et al. 2017). For a given sample, the quality trimmed reads were mapped to the
738 assembled scaffolds using bowtie2 with default parameters (Langmead and Salzberg 2012). The coverage of
739 each scaffold was calculated as the total number of bases mapped to it divided by its length. The protein-
740 coding genes were predicted from the scaffolds using Prodigal (Hyatt et al. 2010), and searched against KEGG,
741 UniRef100 and UniProt for annotation. The 16S rRNA gene was predicted using a HMM model, as previously
742 described (Brown et al. 2015). The tRNAs were predicted using tRNAscan-SE 2.0 (Lowe and Chan 2016). For
743 each sample, scaffolds with a minimum length of 2.5 kbp were assigned to preliminary draft genome bins using
744 MetaBAT with default parameters (Kang et al. 2015), with both tetranucleotide frequencies (TNF) and coverage
745 profile of scaffolds (from multiple samples) considered. The scaffolds from the obtained bins and the unbinned
746 scaffolds with a minimum length of 1 kbp were uploaded to ggKbase (http://ggkbase.berkeley.edu/). The
747 genome bins were evaluated based on the consistency of GC content, coverage and taxonomic information and
748 scaffolds identified as contaminants were removed.
749
750 **GC skew evaluation of RefSeq genomes**
751 We analyzed all the NCBI RefSeq genomes downloaded on May 10th, 2017 for GC Skew. Both skew and
752 cumulative skew were calculated and patterns displayed using the publicly available program gc_skew.py
753 (https://github.com/christophertbrown/iRep) (Brown et al. 2016).
754
755 **Refinement of the CPR genome from blood**
756 For initial characterization of the CPR bin we used the contigs made publicly available as the 'Dataset S6' in the
757 original study (Kowarsky et al. 2017). These contigs represent what remained after the removal of contigs with
758 matches to sequences in any existing public databases (Kowarsky et al. 2017); we will refer to these contigs as
759 'novel contigs'. In our study we also had access to the remaining contigs, and we will refer to this dataset as 'all
760 contigs'.
761 For binning and refinement of the CPR genome, and metagenomic read recruitment analyses, we
762 used anvi'o v5.5 to generate a contigs database from the novel contigs using the program 'anvi-gen-contigs-
763 database', which recovered the tetranucleotide frequencies for each contig, used Prodigal v2.6.3 (Hyatt et al.
764 2010) with default settings to identify open reading frames, and HMMER v3.2.1 (Eddy 2011) to identify
765 matching genes in our contigs to bacterial single-copy core genes by (Campbell et al. 2013). To visualize all
766 novel contigs we used the program 'anvi-interactive', which computed a hierarchical clustering dendrogram for
767 contigs using Euclidean distance and Ward linkage based on their tetranucleotide frequency (TNF), and
768 displayed additional data layers of contig cohort origin and HMM hits we supplied to the program as a TAB-
769 delimited additional data file. We manually selected a branch of contigs that created a coherent cluster based
770 on the TNF data and the occurrence of bacterial single-copy core genes. While this procedure allowed us to
771 identify an initial genome bin with modest completion, it's comprehensiveness and purity was questionable
772 since our binning effort (1) utilized only the novel contigs from the (Kowarsky et al. 2017), which were a subset
773 of all contigs assembled, and (2) only employed tetranucleotide signatures to identify the genome bin, which
774 can introduce contamination as the sequence signatures of short fragments of DNA can be noisy. To address
775 these issues, we first acquired the remaining 3,002 contigs that were not included in the original study
776 (Kowarsky et al. 2017) and that might be derived from the same blood-associated CPR population. Then, we
777 used all blood metagenomes for a read recruitment analysis. This analysis allowed us to identify contigs from
778 the non-novel contig collection that match to the distribution patterns of the initial CPR bin. Since the coverage
779 of this population was extremely low, we used a special clustering configuration for anvi'o to use 'differential
780 detection' rather than 'differential coverage' (see the reproducible workflow for details). This analysis resulted
781 in contigs with similar detection patterns across all metagenomes. We summarized this final collection of

contigs using 'anvi-summarize', which gave access to the FASTA file for the bin. Anvi'o automated workflows (http://merenlab.org/2018/07/09/anvio-snakemake-workflows/) that use snakemake (Köster and Rahmann 2012) performed all read recruitment analyses with Bowtie v2.3.4 (Langmead and Salzberg 2012). We profiled all mapping results using anvi'o following the analysis steps outlined in Eren et al. (Eren et al. 2015).

To put our CPR bin into the phylogenetic context of the other available CPR genomes, we used the 797 metagenome-assembled CPR genomes (Brown et al. 2015). We used the anvi'o program `anvi-get-sequences-for-hmm-hits` to (1) collect the 21 amino acid sequences found in the CPR bin (Ribosomal_L10, Ribosomal_L11, Ribosomal_L11_N, Ribosomal_L13, Ribosomal_L14, Ribosomal_L17, Ribosomal_L20, Ribosomal_L21p, Ribosomal_L27, Ribosomal_L32p, Ribosomal_L5_C, Ribosomal_L9_C, Ribosomal_L9_N, Ribosomal_S11, Ribosomal_S13, Ribosomal_S16, Ribosomal_S2, Ribosomal_S20p, Ribosomal_S4, Ribosomal_S7, Ribosomal_S9) from all genomes, (2) align them individually, (3) concatenate genes that belong to the same genome, and (4) report them as a FASTA file. Some of the key parameters we used with this program included '--hmm-source Campbell_et_al' to use the single-copy core gene collection defined by Campbell et al. (Campbell et al. 2013), '--align-with famsa' to use FAMSA (Deorowicz et al. 2016) to align sequences for each ribosomal protein, '--return-best-hit' to get only the most significant HMM hit if a given ribosomal protein found in multiple copies in a given genome, and '--max-num-genes-missing-from-bin 3' to omit genomes that miss more than 3 of the 21 genes listed. We used trimAl v1.4.rev22 (Capella-Gutiérrez et al. 2009) to remove positions that were gaps in more than 50% of the genes in the alignment (-gt 0.50), IQ-TREE v1.5.5 (Nguyen et al. 2015) with the 'WAG' general matrix model (Whelan and Goldman 2001) to infer the maximum likelihood tree, and anvi'o to visualize the output.

Refinement of the Pasolli MAG

We downloaded the Pasolli MAG ('HMP_2012__SRS023938__bin_39') from http://opendata.lifebit.ai/table/?project=SGB and the 481 HMP oral metagenomes from the HMP FTP server (ftp://public-ftp.hmpdacc.org/Illumina/). We used anvi'o v6 and the Snakemake-based (Köster and Rahmann 2012) program 'anvi-run-workflow' to run the anvi'o metagenomics workflow (Eren et al. 2015)**.** Briefly, we generated a contigs database from the Pasolli MAG FASTA file by running 'anvi-gen-contigs-database', during which anvi'o calculates tetra-nucleotide frequencies for each contig, and Prodigal (Hyatt et al. 2010) to identify genes. In order to estimate the completion and redundancy of the Pasolli MAG based on SCGs, we used the program 'anvi-run-hmms' with the default HMM profiles, which include 71 bacterial SCGs (HMMs described in anvi'o v6), and annotated genes with functions using 'anvi-run-ncbi-cogs' which searches amino-acid sequences using blastp v2.7.1+ (Altschul et al. 1990) against the December 2014 release of the COG database (Tatusov et al. 2000). We mapped the paired-end reads from the 481 HMP metagenomes to the Pasolli MAG using bowtie v2.2.6 with default parameters (Langmead and Salzberg 2012) and converted the mapping output to BAM files using samtools v1.9 (Li et al. 2009). We used 'anvi-profile' to generate profile databases from BAM files, in which coverage and detection statistics for contigs in each metagenome were stored. We used 'anvi-merge' to merge the anvi'o profile databases of (1) only the 3 plaque metagenomes of HMP individual 159268001, which includes the sample from which the Pasolli MAG was constructed (sample accession SRS023938), and (2) all 481 HMP oral metagenomes. In order to manually refine the Pasolli MAG, we ran the anvi'o interactive interface using 'anvi-interactive' with the merged anvi'o profile database that included only the three plaque metagenomes of HMP individual 159268001. Refinement was done using hierarchical clustering of the contigs based on sequence composition and differential coverage using Euclidean distance and Ward's method. To estimate the taxonomic assignment we blasted the protein sequences of genes in the 11 contigs identified as contamination against the NCBI's non-redundant protein sequences database. To visualize the detection values of the contigs of the Pasolli MAG across all 481 HMP oral metagenomes we used the full merged profile database and the program 'anvi-interactive'. We used 'anvi-summarize' to generate tabular summaries of detection and coverage information of the refined Saccharibacteira bin and the 11 contigs of contamination across the 481 metagenomes.

Data access

All sequencing data described in this manuscript is available at the NCBI Genbank under accession numbers provided in Table 1.

Acknowledgements

We thank Brian C. Thomas, Matthew R. Olm, Christopher T. Brown, Alla Lapidus and Christian M.K. Sieber for helpful discussions and Steven Quake and Mark Kowarsky for providing access to unreleased sequences from their cell-free blood study. This work was supported by the Genome Canada Large Scale Applied Research Program and Ontario Research Fund – Research Excellence grants to L.A.W., Lawrence Berkeley National Laboratory's Watershed Function Scientific Focus Area funded by DOE contract DE-AC02-05CH11231, the Office of Science and Office of Biological and Environmental Research (Lawrence Berkeley National Lab; Operated by the University of California, Berkeley) and National Institutes of Health (NIH) under awards RAI092531A and R01-GM109454, Chan Zuckerberg Biohub and the UC Berkeley-based Innovative Genomics Institute.

Disclosure declaration. The authors declare that they have no competing interests.

References

Ackelsberg J, Rakeman J, Hughes S, Petersen J, Mead P, Schriefer M, Kingry L, Hoffmaster A, Gee JE. 2015. Lack of Evidence for Plague or Anthrax on the New York City Subway. *Cell Syst* **1**: 4–5.

Afshinnekoo E, Meydan C, Chowdhury S, Jaroudi D, Boyer C, Bernstein N, Maritz JM, Reeves D, Gandara J, Chhangawala S, et al. 2015. Geospatial Resolution of Human and Bacterial Diversity with City-Scale Metagenomics. *Cell Syst* **1**: 97–97.e3.

Albertsen M, Hugenholtz P, Skarshewski A, Nielsen KL, Tyson GW, Nielsen PH. 2013. Genome sequences of rare, uncultured bacteria obtained by differential coverage binning of multiple metagenomes. *Nat Biotechnol* **31**: 533–538.

Almeida A, Mitchell AL, Boland M, Forster SC, Gloor GB, Tarkowska A, Lawley TD, Finn RD. 2019. A new genomic blueprint of the human gut microbiota. *Nature* **568**: 499–504.

Alneberg J, Bjarnason BS, de Bruijn I, Schirmer M, Quick J, Ijaz UZ, Loman NJ, Andersson AF, Quince C. 2013. CONCOCT: Clustering cONtigs on COverage and ComposiTion. *arXiv [q-bioGN]*. http://arxiv.org/abs/1312.4038.

Al-Shayeb B, Sachdeva R, Chen LX, Ward F, Munk P. 2019. Clades of huge phage from across Earth's ecosystems. *bioRxiv*. https://www.biorxiv.org/content/10.1101/572362v1.abstract.

Altschul SF, Gish W, Miller W, Myers EW, Lipman DJ. 1990. Basic local alignment search tool. *J Mol Biol* **215**: 403–410.

Anantharaman K, Brown CT, Hug LA, Sharon I, Castelle CJ, Probst AJ, Thomas BC, Singh A, Wilkins MJ, Karaoz U, et al. 2016. Thousands of microbial genomes shed light on interconnected biogeochemical processes in an aquifer system. *Nature Communications* **7**. http://dx.doi.org/10.1038/ncomms13219.

Anantharaman K, Hausmann B, Jungbluth SP, Kantor RS, Lavy A, Warren LA, Rappé MS, Pester M, Loy A, Thomas BC, et al. 2018. Expanded diversity of microbial groups that shape the dissimilatory sulfur cycle. *ISME J* **12**: 1715–1728.

Arakawa K. 2016. No evidence for extensive horizontal gene transfer from the draft genome of a tardigrade. *Proc Natl Acad Sci U S A* **113**: E3057.

Arumugam K, Bağcı C, Bessarab I, Beier S, Buchfink B, Górska A, Qiu G, Huson DH, Williams RBH. 2019. Annotated bacterial chromosomes from frame-shift-corrected long-read metagenomic data. *Microbiome* **7**: 61.

Banfield JF, Anantharaman K, Williams KH, Thomas BC. 2017. Complete 4.55-Megabase-Pair Genome of "Candidatus Fluviicola riflensis," Curated from Short-Read Metagenomic Sequences. *Genome Announc* **5**: e01299–17.

Barry ER, Bell SD. 2006. DNA replication in the archaea. *Microbiol Mol Biol Rev* **70**: 876–887.

Baudry L, Foutel-Rodier T, Thierry A, Koszul R, Marbouty M. 2019. MetaTOR: A Computational Pipeline to

882 Recover High-Quality Metagenomic Bins From Mammalian Gut Proximity-Ligation (meta3C) Libraries.
883 *Front Genet* **10**: 753.
884 Becraft ED, Woyke T, Jarett J, Ivanova N, Godoy-Vitorino F, Poulton N, Brown JM, Brown J, Lau MCY, Onstott T,
885 et al. 2017. Rokubacteria: Genomic Giants among the Uncultured Bacterial Phyla. *Front Microbiol* **8**:
886 2264.
887 Bickhart DM, Watson M, Koren S, Panke-Buisse K, Cersosimo LM, Press MO, Van Tassell CP, Van Kessel JAS,
888 Haley BJ, Kim SW, et al. 2019. Assignment of virus and antimicrobial resistance genes to microbial hosts
889 in a complex microbial community by combined long-read assembly and proximity ligation. *Genome*
890 *Biol* **20**: 153.
891 Boothby TC, Tenlen JR, Smith FW, Wang JR, Patanella KA, Nishimura EO, Tintori SC, Li Q, Jones CD, Yandell M,
892 et al. 2015. Evidence for extensive horizontal gene transfer from the draft genome of a tardigrade. *Proc*
893 *Natl Acad Sci U S A* **112**: 15976–15981.
894 Bor B, Bedree JK, Shi W, McLean JS, He X. 2019. Saccharibacteria (TM7) in the Human Oral Microbiome. *J Dent*
895 *Res* **98**: 500–509.
896 Bowers RM, Kyrpides NC, Stepanauskas R, Harmon-Smith M, Doud D, Reddy TBK, Schulz F, Jarett J, Rivers AR,
897 Eloe-Fadrosh EA, et al. 2017. Minimum information about a single amplified genome (MISAG) and a
898 metagenome-assembled genome (MIMAG) of bacteria and archaea. *Nat Biotechnol* **35**: 725.
899 Brooks B, Olm MR, Firek BA, Baker R, Thomas BC, Morowitz MJ, Banfield JF. 2017. Strain-resolved analysis of
900 hospital rooms and infants reveals overlap between the human and room microbiome. *Nat Commun* **8**:
901 1814.
902 Brown CT, Hug LA, Thomas BC, Sharon I, Castelle CJ, Singh A, Wilkins MJ, Wrighton KC, Williams KH, Banfield
903 JF. 2015. Unusual biology across a group comprising more than 15% of domain Bacteria. *Nature* **523**:
904 208–211.
905 Brown CT, Olm MR, Thomas BC, Banfield JF. 2016. Measurement of bacterial replication rates in microbial
906 communities. *Nat Biotechnol* **34**: 1256–1263.
907 Bushnell B. 2018. BBTools: a suite of fast, multithreaded bioinformatics tools designed for analysis of DNA and
908 RNA sequence data. *Joint Genome Institute https://jgi doe gov/data-and-tools/bbtools*.
909 Campbell JH, O'Donoghue P, Campbell AG, Schwientek P, Sczyrba A, Woyke T, Söll D, Podar M. 2013. UGA is
910 an additional glycine codon in uncultured SR1 bacteria from the human microbiota. *Proc Natl Acad Sci*
911 *U S A* **110**: 5540–5545.
912 Capella-Gutiérrez S, Silla-Martínez JM, Gabaldón T. 2009. trimAl: a tool for automated alignment trimming in
913 large-scale phylogenetic analyses. *Bioinformatics* **25**: 1972–1973.
914 Castelle CJ, Hug LA, Wrighton KC, Thomas BC, Williams KH, Wu D, Tringe SG, Singer SW, Eisen JA, Banfield JF.
915 2013. Extraordinary phylogenetic diversity and metabolic versatility in aquifer sediment. *Nature*
916 *Communications* **4**. http://dx.doi.org/10.1038/ncomms3120.
917 Chen LX, Zhao YL, McMahon KD, Mori JF, Jessen GL. 2019. Wide distribution of phage that infect freshwater
918 SAR11 bacteria. *bioRxiv*. https://www.biorxiv.org/content/10.1101/672428v1.abstract.
919 Chivian D, Brodie EL, Alm EJ, Culley DE, Dehal PS, DeSantis TZ, Gihring TM, Lapidus A, Lin L-H, Lowry SR, et al.
920 2008. Environmental genomics reveals a single-species ecosystem deep within Earth. *Science* **322**: 275–
921 278.
922 Daims H, Lebedeva EV, Pjevac P, Han P, Herbold C, Albertsen M, Jehmlich N, Palatinszky M, Vierheilig J, Bulaev
923 A, et al. 2015. Complete nitrification by Nitrospira bacteria. *Nature* **528**: 504.
924 Dekker J, Rippe K, Dekker M, Kleckner N. 2002. Capturing chromosome conformation. *Science* **295**: 1306–
925 1311.
926 Delmont TO, Eren AM. 2016. Identifying contamination with advanced visualization and analysis practices:
927 metagenomic approaches for eukaryotic genome assemblies. *PeerJ* **4**: e1839.
928 Delmont TO, Kiefl E, Kilinc O, Esen OC, Uysal I, Rappé MS, Giovannoni S, Eren AM. 2019. Single-amino acid
929 variants reveal evolutionary processes that shape the biogeography of a global SAR11 subclade. *Elife* **8**.
930 http://dx.doi.org/10.7554/eLife.46497.
931 Delmont TO, Quince C, Shaiber A, Esen ÖC, Lee ST, Rappé MS, McLellan SL, Lücker S, Eren AM. 2018. Nitrogen-

932 fixing populations of Planctomycetes and Proteobacteria are abundant in surface ocean metagenomes.
933 *Nat Microbiol* **3**: 804–813.
934 DeMaere MZ, Darling AE. 2019. bin3C: exploiting Hi-C sequencing data to accurately resolve metagenome-
935 assembled genomes. *Genome Biology* **20**. http://dx.doi.org/10.1186/s13059-019-1643-1.
936 Deorowicz S, Debudaj-Grabysz A, Gudyś A. 2016. FAMSA: Fast and accurate multiple sequence alignment of
937 huge protein families. *Sci Rep* **6**: 33964.
938 Devoto AE, Santini JM, Olm MR, Anantharaman K, Munk P, Tung J, Archie EA, Turnbaugh PJ, Seed KD,
939 Blekhman R, et al. 2019. Megaphages infect Prevotella and variants are widespread in gut microbiomes.
940 *Nat Microbiol* **4**: 693–700.
941 Di Rienzi SC, Sharon I, Wrighton KC, Koren O, Hug LA, Thomas BC, Goodrich JK, Bell JT, Spector TD, Banfield JF,
942 et al. 2013. The human gut and groundwater harbor non-photosynthetic bacteria belonging to a new
943 candidate phylum sibling to Cyanobacteria. *Elife* **2**: e01102.
944 Driscoll CB, Otten TG, Brown NM, Dreher TW. 2017. Towards long-read metagenomics: complete assembly of
945 three novel genomes from bacteria dependent on a diazotrophic cyanobacterium in a freshwater lake
946 co-culture. *Standards in Genomic Sciences* **12**. http://dx.doi.org/10.1186/s40793-017-0224-8.
947 Eddy SR. 2011. Accelerated Profile HMM Searches. *PLoS Comput Biol* **7**: e1002195.
948 Eisen JA, Heidelberg JF, White O, Salzberg SL. 2000. Evidence for symmetric chromosomal inversions around
949 the replication origin in bacteria. *Genome Biol* **1**: RESEARCH0011.
950 Eren AM, Borisy GG, Huse SM, Mark Welch JL. 2014. Oligotyping analysis of the human oral microbiome. *Proc*
951 *Natl Acad Sci U S A* **111**: E2875–84.
952 Eren AM, Esen ÖC, Quince C, Vineis JH, Morrison HG, Sogin ML, Delmont TO. 2015. Anvi'o: an advanced
953 analysis and visualization platform for 'omics data. *PeerJ* **3**: e1319.
954 Fraser CM, Eisen JA, Nelson KE, Paulsen IT, Salzberg SL. 2002. The value of complete microbial genome
955 sequencing (you get what you pay for). *J Bacteriol* **184**: 6403–6405.
956 Garcia SL, Stevens SLR, Crary B, Martinez-Garcia M, Stepanauskas R, Woyke T, Tringe SG, Andersson SGE,
957 Bertilsson S, Malmstrom RR, et al. 2018. Contrasting patterns of genome-level diversity across distinct
958 co-occurring bacterial populations. *ISME J* **12**: 742–755.
959 Garg SG, Kapust N, Lin W, Tria FDK, Nelson-Sathi S, Gould SB, Fan L, Zhu R, Zhang C, Martin WF. 2019.
960 Anomalous phylogenetic behavior of ribosomal proteins in metagenome assembled genomes. *bioRxiv*
961 731091. https://www.biorxiv.org/content/10.1101/731091v1.abstract (Accessed August 15, 2019).
962 Giovannoni SJ. 2017. SAR11 Bacteria: The Most Abundant Plankton in the Oceans. *Ann Rev Mar Sci* **9**: 231–
963 255.
964 Greenwald WW, Klitgord N, Seguritan V, Yooseph S, Venter JC, Garner C, Nelson KE, Li W. 2017. Utilization of
965 defined microbial communities enables effective evaluation of meta-genomic assemblies. *BMC*
966 *Genomics* **18**: 296.
967 Grigoriev A. 1998. Analyzing genomes with cumulative skew diagrams. *Nucleic Acids Res* **26**: 2286–2290.
968 He X, McLean JS, Edlund A, Yooseph S, Hall AP, Liu S-Y, Dorrestein PC, Esquenazi E, Hunter RC, Cheng G, et al.
969 2015. Cultivation of a human-associated TM7 phylotype reveals a reduced genome and epibiotic
970 parasitic lifestyle. *Proc Natl Acad Sci U S A* **112**: 244–249.
971 Hongoh Y, Sharma VK, Prakash T, Noda S, Taylor TD, Kudo T, Sakaki Y, Toyoda A, Hattori M, Ohkuma M. 2008.
972 Complete genome of the uncultured Termite Group 1 bacteria in a single host protist cell. *Proc Natl*
973 *Acad Sci U S A* **105**: 5555–5560.
974 Hug LA, Baker BJ, Anantharaman K, Brown CT, Probst AJ, Castelle CJ, Butterfield CN, Hernsdorf AW, Amano Y,
975 Ise K, et al. 2016. A new view of the tree of life. *Nat Microbiol* **1**: 16048.
976 Hyatt D, Chen G-L, Locascio PF, Land ML, Larimer FW, Hauser LJ. 2010. Prodigal: prokaryotic gene recognition
977 and translation initiation site identification. *BMC Bioinformatics* **11**: 119.
978 Iverson V, Morris RM, Frazar CD, Berthiaume CT, Morales RL, Armbrust EV. 2012. Untangling genomes from
979 metagenomes: revealing an uncultured class of marine Euryarchaeota. *Science* **335**: 587–590.
980 Kalisky T, Quake SR. 2011. Single-cell genomics. *Nat Methods* **8**: 311–314.
981 Kang DD, Froula J, Egan R, Wang Z. 2015. MetaBAT, an efficient tool for accurately reconstructing single

982 genomes from complex microbial communities. *PeerJ* **3**: e1165.
983 Kantor RS, Huddy RJ, Iyer R, Thomas BC, Brown CT, Anantharaman K, Tringe S, Hettich RL, Harrison STL,
984 Banfield JF. 2017. Genome-Resolved Meta-Omics Ties Microbial Dynamics to Process Performance in
985 Biotechnology for Thiocyanate Degradation. *Environ Sci Technol* **51**: 2944–2953.
986 Kantor RS, Wrighton KC, Handley KM, Sharon I, Hug LA, Castelle CJ, Thomas BC, Banfield JF. 2013. Small
987 genomes and sparse metabolisms of sediment-associated bacteria from four candidate phyla. *MBio* **4**:
988 e00708–13.
989 Kashtan N, Roggensack SE, Rodrigue S, Thompson JW, Biller SJ, Coe A, Ding H, Marttinen P, Malmstrom RR,
990 Stocker R, et al. 2014. Single-cell genomics reveals hundreds of coexisting subpopulations in wild
991 Prochlorococcus. *Science* **344**: 416–420.
992 Kearse M, Moir R, Wilson A, Stones-Havas S, Cheung M, Sturrock S, Buxton S, Cooper A, Markowitz S, Duran C,
993 et al. 2012. Geneious Basic: an integrated and extendable desktop software platform for the
994 organization and analysis of sequence data. *Bioinformatics* **28**: 1647–1649.
995 Korem T, Zeevi D, Suez J, Weinberger A, Avnit-Sagi T, Pompan-Lotan M, Matot E, Jona G, Harmelin A, Cohen N,
996 et al. 2015. Growth dynamics of gut microbiota in health and disease inferred from single metagenomic
997 samples. *Science* **349**: 1101–1106.
998 Köster J, Rahmann S. 2012. Snakemake--a scalable bioinformatics workflow engine. *Bioinformatics* **28**: 2520–
999 2522.
1000 Kowarsky M, Camunas-Soler J, Kertesz M, De Vlaminck I, Koh W, Pan W, Martin L, Neff NF, Okamoto J, Wong
1001 RJ, et al. 2017. Numerous uncharacterized and highly divergent microbes which colonize humans are
1002 revealed by circulating cell-free DNA. *Proc Natl Acad Sci U S A*.
1003 http://dx.doi.org/10.1073/pnas.1707009114.
1004 Labonté JM, Swan BK, Poulos B, Luo H, Koren S, Hallam SJ, Sullivan MB, Woyke T, Eric Wommack K,
1005 Stepanauskas R. 2015. Single-cell genomics-based analysis of virus–host interactions in marine surface
1006 bacterioplankton. *ISME J* **9**: 2386–2399.
1007 Laczny CC, Sternal T, Plugaru V, Gawron P, Atashpendar A, Margossian HH, Coronado S, van der Maaten L,
1008 Vlassis N, Wilmes P. 2015. VizBin - an application for reference-independent visualization and human-
1009 augmented binning of metagenomic data. *Microbiome* **3**: 1.
1010 Langmead B, Salzberg SL. 2012. Fast gapped-read alignment with Bowtie 2. *Nat Methods* **9**: 357–359.
1011 Laver T, Harrison J, O'Neill PA, Moore K, Farbos A, Paszkiewicz K, Studholme DJ. 2015. Assessing the
1012 performance of the Oxford Nanopore Technologies MinION. *Biomol Detect Quantif* **3**: 1–8.
1013 Le TBK, Imakaev MV, Mirny LA, Laub MT. 2013. High-resolution mapping of the spatial organization of a
1014 bacterial chromosome. *Science* **342**: 731–734.
1015 Lieberman-Aiden E, van Berkum NL, Williams L, Imakaev M, Ragoczy T, Telling A, Amit I, Lajoie BR, Sabo PJ,
1016 Dorschner MO, et al. 2009. Comprehensive mapping of long-range interactions reveals folding
1017 principles of the human genome. *Science* **326**: 289–293.
1018 Li H, Handsaker B, Wysoker A, Fennell T, Ruan J, Homer N, Marth G, Abecasis G, Durbin R, 1000 Genome
1019 Project Data Processing Subgroup. 2009. The Sequence Alignment/Map format and SAMtools.
1020 *Bioinformatics* **25**: 2078–2079.
1021 Liu M, Darling A. 2015. Metagenomic Chromosome Conformation Capture (3C): techniques, applications, and
1022 challenges. *F1000Res* **4**: 1377.
1023 Lobry JR. 1996. Origin of replication of Mycoplasma genitalium. *Science* **272**: 745–746.
1024 Lo I, Denef VJ, Verberkmoes NC, Shah MB, Goltsman D, DiBartolo G, Tyson GW, Allen EE, Ram RJ, Detter JC, et
1025 al. 2007. Strain-resolved community proteomics reveals recombining genomes of acidophilic bacteria.
1026 *Nature* **446**: 537–541.
1027 Lowe TM, Chan PP. 2016. tRNAscan-SE On-line: integrating search and context for analysis of transfer RNA
1028 genes. *Nucleic Acids Res* **44**: W54–7.
1029 Luef B, Frischkorn KR, Wrighton KC, Holman H-YN, Birarda G, Thomas BC, Singh A, Williams KH, Siegerist CE,
1030 Tringe SG, et al. 2015. Diverse uncultivated ultra-small bacterial cells in groundwater. *Nat Commun* **6**:
1031 6372.

1032 Marbouty M, Cournac A, Flot J-F, Marie-Nelly H, Mozziconacci J, Koszul R. 2014. Metagenomic chromosome
1033 conformation capture (meta3C) unveils the diversity of chromosome organization in microorganisms.
1034 *Elife* **3**: e03318.
1035 Marbouty M, Koszul R. 2015. Metagenome Analysis Exploiting High-Throughput Chromosome Conformation
1036 Capture (3C) Data. *Trends in Genetics* **31**: 673–682. http://dx.doi.org/10.1016/j.tig.2015.10.003.
1037 Mark Welch JL, Utter DR, Rossetti BJ, Mark Welch DB, Eren AM, Borisy GG. 2014. Dynamics of tongue
1038 microbial communities with single-nucleotide resolution using oligotyping. *Front Microbiol* **5**: 568.
1039 Mosier AC, Miller CS, Frischkorn KR, Ohm RA, Li Z, LaButti K, Lapidus A, Lipzen A, Chen C, Johnson J, et al.
1040 2016. Fungi Contribute Critical but Spatially Varying Roles in Nitrogen and Carbon Cycling in Acid Mine
1041 Drainage. *Frontiers in Microbiology* **7**. http://dx.doi.org/10.3389/fmicb.2016.00238.
1042 Moustafa A, Xie C, Kirkness E, Biggs W, Wong E, Turpaz Y, Bloom K, Delwart E, Nelson KE, Venter JC, et al.
1043 2017. The blood DNA virome in 8,000 humans. *PLoS Pathog* **13**: e1006292.
1044 Nadalin F, Vezzi F, Policriti A. 2012. GapFiller: a de novo assembly approach to fill the gap within paired reads.
1045 *BMC Bioinformatics* **13 Suppl 14**: S8.
1046 Nakamura Y. 2002. Complete Genome Structure of the Thermophilic Cyanobacterium Thermosynechococcus
1047 elongatus BP-1. *DNA Research* **9**: 123–130. http://dx.doi.org/10.1093/dnares/9.4.123.
1048 Nayfach S, Shi ZJ, Seshadri R, Pollard KS, Kyrpides N. 2019. Novel insights from uncultivated genomes of the
1049 global human gut microbiome. *Nature*. http://dx.doi.org/10.1038/s41586-019-1058-x.
1050 Nelson WC, Stegen JC. 2015. The reduced genomes of Parcubacteria (OD1) contain signatures of a symbiotic
1051 lifestyle. *Front Microbiol* **6**: 713.
1052 Newton RJ, Jones SE, Helmus MR, McMahon KD. 2007. Phylogenetic ecology of the freshwater Actinobacteria
1053 acI lineage. *Appl Environ Microbiol* **73**: 7169–7176.
1054 Nguyen L-T, Schmidt HA, von Haeseler A, Minh BQ. 2015. IQ-TREE: a fast and effective stochastic algorithm for
1055 estimating maximum-likelihood phylogenies. *Mol Biol Evol* **32**: 268–274.
1056 Nicholls SM, Quick JC, Tang S, Loman NJ. 2019. Ultra-deep, long-read nanopore sequencing of mock microbial
1057 community standards. *Gigascience* **8**. http://dx.doi.org/10.1093/gigascience/giz043.
1058 Nurk S, Meleshko D, Korobeynikov A, Pevzner PA. 2017. metaSPAdes: a new versatile metagenomic
1059 assembler. *Genome Res* **27**: 824–834.
1060 Olm MR, Brown CT, Brooks B, Firek B, Baker R, Burstein D, Soenjoyo K, Thomas BC, Morowitz M, Banfield JF.
1061 2017. Identical bacterial populations colonize premature infant gut, skin, and oral microbiomes and
1062 exhibit different in situ growth rates. *Genome Res* **27**: 601–612.
1063 Olm MR, West PT, Brooks B, Firek BA, Baker R, Morowitz MJ, Banfield JF. 2019. Genome-resolved
1064 metagenomics of eukaryotic populations during early colonization of premature infants and in hospital
1065 rooms. *Microbiome* **7**: 26.
1066 Olson ND, Treangen TJ, Hill CM, Cepeda-Espinoza V, Ghurye J, Koren S, Pop M. 2017. Metagenomic assembly
1067 through the lens of validation: recent advances in assessing and improving the quality of genomes
1068 assembled from metagenomes. *Brief Bioinform*. http://dx.doi.org/10.1093/bib/bbx098.
1069 Parks DH, Chuvochina M, Waite DW, Rinke C, Skarshewski A, Chaumeil P-A, Hugenholtz P. 2018. A
1070 standardized bacterial taxonomy based on genome phylogeny substantially revises the tree of life. *Nat*
1071 *Biotechnol* **36**: 996–1004.
1072 Parks DH, Imelfort M, Skennerton CT, Hugenholtz P, Tyson GW. 2015. CheckM: assessing the quality of
1073 microbial genomes recovered from isolates, single cells, and metagenomes. *Genome Res* **25**: 1043–
1074 1055.
1075 Parks DH, Rinke C, Chuvochina M, Chaumeil P-A, Woodcroft BJ, Evans PN, Hugenholtz P, Tyson GW. 2017.
1076 Recovery of nearly 8,000 metagenome-assembled genomes substantially expands the tree of life. *Nat*
1077 *Microbiol* **2**: 1533–1542.
1078 Pasolli E, Asnicar F, Manara S, Zolfo M, Karcher N, Armanini F, Beghini F, Manghi P, Tett A, Ghensi P, et al.
1079 2019. Extensive Unexplored Human Microbiome Diversity Revealed by Over 150,000 Genomes from
1080 Metagenomes Spanning Age, Geography, and Lifestyle. *Cell* **176**: 649–662.e20.
1081 Pelletier E, Kreimeyer A, Bocs S, Rouy Z, Gyapay G, Chouari R, Rivière D, Ganesan A, Daegelen P, Sghir A, et al.

1082 2008. “Candidatus Cloacamonas Acidaminovorans”: Genome Sequence Reconstruction Provides a First
1083 Glimpse of a New Bacterial Division. *J Bacteriol* **190**: 2572–2579.
1084 Peng Y, Leung HCM, Yiu SM, Chin FYL. 2012. IDBA-UD: a de novo assembler for single-cell and metagenomic
1085 sequencing data with highly uneven depth. *Bioinformatics* **28**: 1420–1428.
1086 Probst AJ, Banfield JF. 2018. Homologous Recombination and Transposon Propagation Shape the Population
1087 Structure of an Organism from the Deep Subsurface with Minimal Metabolism. *Genome Biol Evol* **10**:
1088 1115–1119.
1089 Probst AJ, Ladd B, Jarett JK, Geller-McGrath DE, Sieber CMK, Emerson JB, Anantharaman K, Thomas BC,
1090 Malmstrom RR, Stieglmeier M, et al. 2018. Differential depth distribution of microbial function and
1091 putative symbionts through sediment-hosted aquifers in the deep terrestrial subsurface. *Nat Microbiol*
1092 **3**: 328–336.
1093 Quandt CA, Alisha Quandt C, Kohler A, Hesse CN, Sharpton TJ, Martin F, Spatafora JW. 2015. Metagenome
1094 sequence of Elaphomyces granulatus from sporocarp tissue reveals Ascomycota ectomycorrhizal
1095 fingerprints of genome expansion and aProteobacteria-rich microbiome. *Environmental Microbiology*
1096 **17**: 2952–2968. http://dx.doi.org/10.1111/1462-2920.12840.
1097 Quince C, Delmont TO, Raguideau S, Alneberg J, Darling AE, Collins G, Eren AM. 2017. DESMAN: a new tool for
1098 de novo extraction of strains from metagenomes. *Genome Biol* **18**: 181.
1099 Rang FJ, Kloosterman WP, de Ridder J. 2018. From squiggle to basepair: computational approaches for
1100 improving nanopore sequencing read accuracy. *Genome Biol* **19**: 90.
1101 Rao SSP, Huntley MH, Durand NC, Stamenova EK, Bochkov ID, Robinson JT, Sanborn AL, Machol I, Omer AD,
1102 Lander ES, et al. 2014. A 3D map of the human genome at kilobase resolution reveals principles of
1103 chromatin looping. *Cell* **159**: 1665–1680.
1104 Raveh-Sadka T, Thomas BC, Singh A, Firek B, Brooks B, Castelle CJ, Sharon I, Baker R, Good M, Morowitz MJ, et
1105 al. 2015. Gut bacteria are rarely shared by co-hospitalized premature infants, regardless of necrotizing
1106 enterocolitis development. *Elife* **4**. http://dx.doi.org/10.7554/eLife.05477.
1107 Reveillaud J, Bordenstein SR, Cruaud C, Shaiber A, Esen ÖC, Weill M, Makoundou P, Lolans K, Watson AR,
1108 Rakotoarivony I, et al. 2019. The Wolbachia mobilome in Culex pipiens includes a putative plasmid. *Nat*
1109 *Commun* **10**: 1051.
1110 Rinke C, Schwientek P, Sczyrba A, Ivanova NN, Anderson IJ, Cheng J-F, Darling A, Malfatti S, Swan BK, Gies EA,
1111 et al. 2013. Insights into the phylogeny and coding potential of microbial dark matter. *Nature* **499**: 431–
1112 437.
1113 Robinson JT, Thorvaldsdóttir H, Winckler W, Guttman M, Lander ES, Getz G, Mesirov JP. 2011. Integrative
1114 genomics viewer. *Nat Biotechnol* **29**: 24.
1115 Rocha EP, Danchin A, Viari A. 1999. Universal replication biases in bacteria. *Mol Microbiol* **32**: 11–16.
1116 Rojas-Carulla M, Ley RE, Schölkopf B, Youngblut ND. 2019. DeepMAsED: Evaluating the quality of
1117 metagenomic assemblies. http://dx.doi.org/10.1101/763813.
1118 Roux S, Enault F, Hurwitz BL, Sullivan MB. 2015. VirSorter: mining viral signal from microbial genomic data.
1119 *PeerJ* **3**: e985.
1120 Sangwan N, Xia F, Gilbert JA. 2016. Recovering complete and draft population genomes from metagenome
1121 datasets. *Microbiome* **4**: 8.
1122 Schirmer M, D’Amore R, Ijaz UZ, Hall N, Quince C. 2016. Illumina error profiles: resolving fine-scale variation in
1123 metagenomic sequencing data. *BMC Bioinformatics* **17**: 125.
1124 Shaiber A, Eren AM. 2019. Composite Metagenome-Assembled Genomes Reduce the Quality of Public
1125 Genome Repositories. *MBio* **10**. http://dx.doi.org/10.1128/mBio.00725-19.
1126 Sharon I, Banfield JF. 2013. Genomes from Metagenomics. *Science* **342**: 1057–1058.
1127 Sharon I, Morowitz MJ, Thomas BC, Costello EK, Relman DA, Banfield JF. 2013. Time series community
1128 genomics analysis reveals rapid shifts in bacterial species, strains, and phage during infant gut
1129 colonization. *Genome Research* **23**: 111–120. http://dx.doi.org/10.1101/gr.142315.112.
1130 Sieber CMK, Probst AJ, Sharrar A, Thomas BC, Hess M, Tringe SG, Banfield JF. 2018. Recovery of genomes from
1131 metagenomes via a dereplication, aggregation and scoring strategy. *Nat Microbiol* **3**: 836–843.

1132 Simmons SL, Dibartolo G, Denef VJ, Goltsman DSA, Thelen MP, Banfield JF. 2008. Population genomic analysis
1133 of strain variation in Leptospirillum group II bacteria involved in acid mine drainage formation. *PLoS Biol*
1134 **6**: e177.
1135 Stalder T, Press MO, Sullivan S, Liachko I, Top EM. 2019. Linking the resistome and plasmidome to the
1136 microbiome. *ISME J* **13**: 2437–2446.
1137 Stepanauskas R. 2012. Single cell genomics: an individual look at microbes. *Curr Opin Microbiol* **15**: 613–620.
1138 Swan BK, Martinez-Garcia M, Preston CM, Sczyrba A, Woyke T, Lamy D, Reinthaler T, Poulton NJ, Masland
1139 EDP, Gomez ML, et al. 2011. Potential for chemolithoautotrophy among ubiquitous bacteria lineages in
1140 the dark ocean. *Science* **333**: 1296–1300.
1141 Tatusov RL, Galperin MY, Natale DA, Koonin EV. 2000. The COG database: a tool for genome-scale analysis of
1142 protein functions and evolution. *Nucleic Acids Res* **28**: 33–36.
1143 Tully BJ, Graham ED, Heidelberg JF. 2018. The reconstruction of 2,631 draft metagenome-assembled genomes
1144 from the global oceans. *Sci Data* **5**: 170203.
1145 Turnbaugh PJ, Ley RE, Hamady M, Fraser-Liggett CM, Knight R, Gordon JI. 2007. The human microbiome
1146 project. *Nature* **449**: 804–810.
1147 Tyson GW, Chapman J, Hugenholtz P, Allen EE, Ram RJ, Richardson PM, Solovyev VV, Rubin EM, Rokhsar DS,
1148 Banfield JF. 2004. Community structure and metabolism through reconstruction of microbial genomes
1149 from the environment. *Nature* **428**: 37–43.
1150 Uritskiy GV, DiRuggiero J, Taylor J. 2018. MetaWRAP—a flexible pipeline for genome-resolved metagenomic
1151 data analysis. *Microbiome* **6**: 158.
1152 van Kessel MAHJ, Speth DR, Albertsen M, Nielsen PH, Op den Camp HJM, Kartal B, Jetten MSM, Lücker S.
1153 2015. Complete nitrification by a single microorganism. *Nature* **528**: 555–559.
1154 Vineis JH, Ringus DL, Morrison HG, Delmont TO, Dalal S, Raffals LH, Antonopoulos DA, Rubin DT, Eren AM,
1155 Chang EB, et al. 2016. Patient-Specific Bacteroides Genome Variants in Pouchitis. *MBio* **7**.
1156 http://dx.doi.org/10.1128/mBio.01713-16.
1157 West PT, Probst AJ, Grigoriev IV, Thomas BC, Banfield JF. 2018. Genome-reconstruction for eukaryotes from
1158 complex natural microbial communities. *Genome Res* **28**: 569–580.
1159 Whelan S, Goldman N. 2001. A general empirical model of protein evolution derived from multiple protein
1160 families using a maximum-likelihood approach. *Mol Biol Evol* **18**: 691–699.
1161 White RA 3rd, Bottos EM, Roy Chowdhury T, Zucker JD, Brislawn CJ, Nicora CD, Fansler SJ, Glaesemann KR,
1162 Glass K, Jansson JK. 2016. Moleculo Long-Read Sequencing Facilitates Assembly and Genomic Binning
1163 from Complex Soil Metagenomes. *mSystems* **1**. http://dx.doi.org/10.1128/mSystems.00045-16.
1164 Wick RR, Judd LM, Gorrie CL, Holt KE. 2017. Unicycler: Resolving bacterial genome assemblies from short and
1165 long sequencing reads. *PLoS Comput Biol* **13**: e1005595.
1166 Woyke T, Doud DFR, Schulz F. 2017. The trajectory of microbial single-cell sequencing. *Nat Methods* **14**: 1045–
1167 1054.
1168 Woyke T, Tighe D, Mavromatis K, Clum A, Copeland A, Schackwitz W, Lapidus A, Wu D, McCutcheon JP,
1169 McDonald BR, et al. 2010. One Bacterial Cell, One Complete Genome. *PLoS ONE* **5**: e10314.
1170 http://dx.doi.org/10.1371/journal.pone.0010314.
1171 Wrighton KC, Thomas BC, Sharon I, Miller CS, Castelle CJ, VerBerkmoes NC, Wilkins MJ, Hettich RL, Lipton MS,
1172 Williams KH, et al. 2012. Fermentation, hydrogen, and sulfur metabolism in multiple uncultivated
1173 bacterial phyla. *Science* **337**: 1661–1665.
1174 Wu D, Hugenholtz P, Mavromatis K, Pukall R, Dalin E, Ivanova NN, Kunin V, Goodwin L, Wu M, Tindall BJ, et al.
1175 2009. A phylogeny-driven genomic encyclopaedia of Bacteria and Archaea. *Nature* **462**: 1056–1060.
1176 Wu Y-W, Tang Y-H, Tringe SG, Simmons BA, Singer SW. 2014. MaxBin: an automated binning method to
1177 recover individual genomes from metagenomes using an expectation-maximization algorithm.
1178 *Microbiome* **2**: 26.